Physical Scaling of Tocardo's Eastern Scheldt Turbines

Additional Graduation Work

B.J. van de Zande

Delft University of Technology

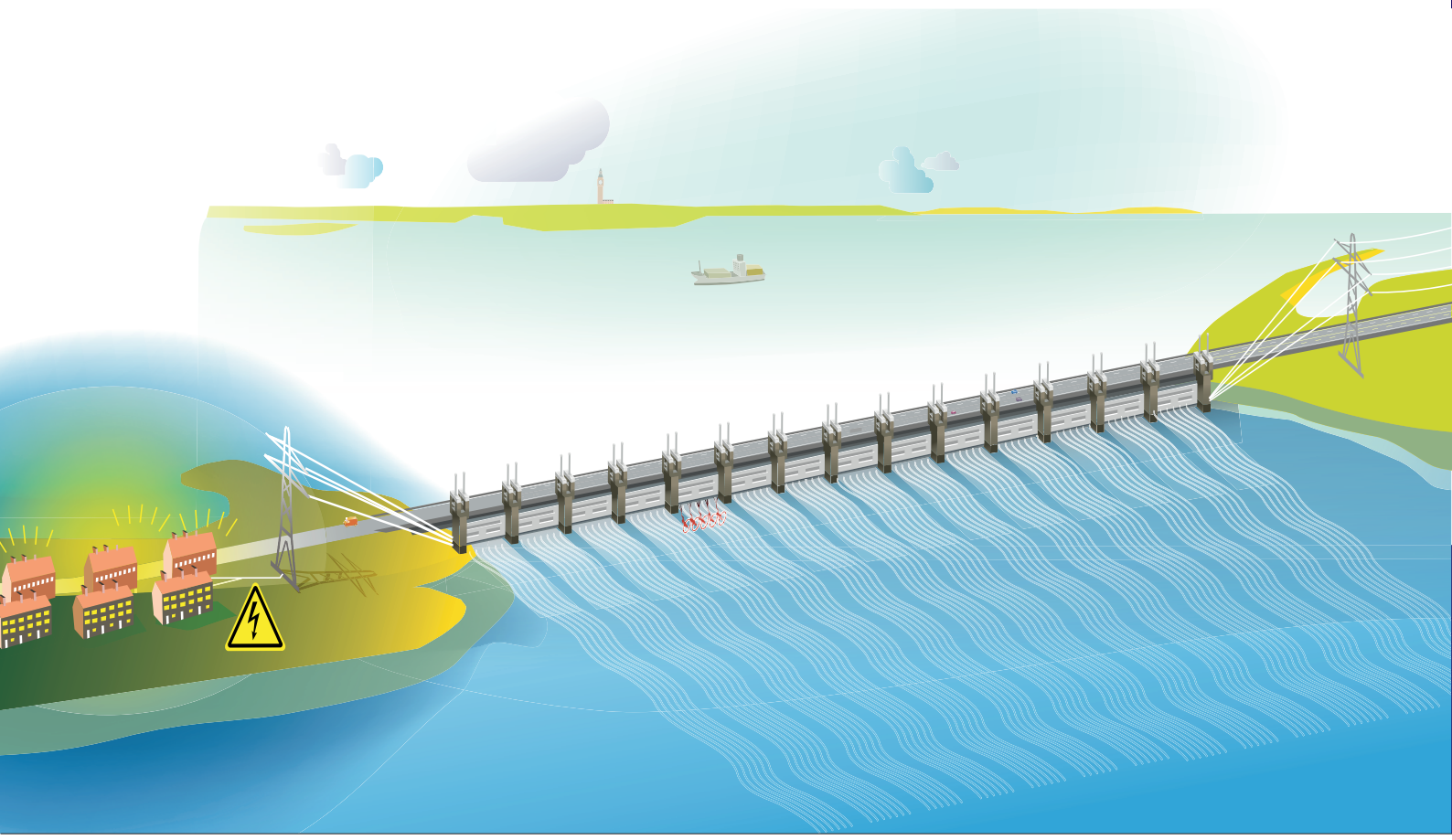

TU Delft Delft University of Technology

Challenge the future

Physical Scaling of Tocardo's Eastern Scheldt Turbines

Additional Graduation Work

by

B.J. van de Zande

in partial fulfillment of the requirements for the degree of

Master of Science
in Hydraulic Engineering

at the Delft University of Technology, Faculty of Civil Engineering and Geosciences

Student number:	4160207	
Project duration:	February 20, 2017 – June 1, 2017	
Thesis committee:	Prof. dr. ir. W.S.J. Uijttewaal,	TU Delft
	Dr. ir. R.J. Labeur,	TU Delft
	MSc. M.C. Verbeek,	TU Delft

An electronic version of this thesis is available at http://repository.tudelft.nl/.

Cover image: Artist impression of tidal energy extraction in the Eastern Scheldt, The Netherlands (source: Jaarbericht Rijkswaterstaat 2015, p. 39)

TU Delft Delft University of Technology

Preface

This additional graduation work is submitted as part of the Master's program Hydraulic Engineering at Delft University of Technology.

I am convinced that, if humanity wants to maintain the quality of life that is experienced today, we should invest in more sustainable forms of energy generation. The subject of tidal energy extraction has drawn my attention since the power of water fascinates me. With this additional graduation work I hope to contribute to the knowledge that is being developed in the field of tidal energy.

I would like to thank the members of this additional thesis committee prof. dr. ir. W.S.J. Uijttewaal, dr. ir. R.J. Labeur and MSc M.C. Verbeek for the feedback and guidance throughout this research. I owe a special word of thanks to Merel Verbeek, who provided me with this subject and was always open to answer my questions. I wish her all the best during her PhD research.

Furthermore, I would like to acknowledge Tocardo International BV for providing the data that was used in this report.

Finally, I would like to thank the Project Ladysmith group with whom I have participated in a multidisciplinary MSc project in South Africa earlier this academic year. These fellow students have, in a short period of time, become good friends and were the best distraction when needed.

B.J. van de Zande
Delft, June 2017

Summary

The largest structure of the Dutch Delta Works, that protect the Netherlands against high water levels at sea, is the Eastern Scheldt storm surge barrier. The Eastern Scheldt barrier is constructed as an open structure that can separate the Eastern Scheldt estuary from the North Sea. In case that water levels of +3.00 m NAP are expected, the steel gates of the barrier close and the hinterland is protected against floods. Besides the protective function of the barrier, the location also shows potential for tidal energy extraction.

Since November 2015, Tocardo International BV has installed five Horizontal Axis Tidal Turbines in the Eastern Scheldt storm surge barrier. These tidal stream turbines have a total capacity of 1.25 MW and satisfy the energy demand of 1000 Dutch households. The Eastern Scheldt barrier is convenient for energy extraction due to the high flow velocities through the structure's gates, and can be equipped with more tidal stream turbines. However, before expansion of tidal energy extraction at this location can be considered, it should clearly be understood what the effects are on the Eastern Scheldt barrier and the environment. Research including experiments with scaled tidal stream turbines can be useful to obtain insight into these matters.

The main goal of this additional graduation work is to determine the scaling parameters for a physical scale model of Tocardo's Horizontal Axis Tidal Turbines in the Eastern Scheldt storm surge barrier, that can be used in open channel experiments in the water laboratory of Delft University of Technology. The physical scale model will be used by a research group of the section Environmental Fluid Mechanics that currently investigates the possible hydro-environmental effects of the installed turbines. In this report recommendations will be proposed that improve the design of a downscaled turbine model.

In order to design a physical scale model, several methods have been discussed that were used in literature to obtain model-prototype similarity. In this report the reader is informed about the following methods: inpectional analysis, the Buckingham Pi theorem, calibration and scale series. Additionally, from the results of previous experiments with mesh disk simulators and physical scaled turbine models it was learned that various factors affect the flow downstream of tidal stream turbines. Factors that should be taken into account in the design of a physical scale model are the thrust coefficient, vertical position of the model, bed roughness, turbine's support structure, ambient turbulence intensity, lateral boundaries and surface waves. The given literature review ends with a introduction to Blade Element Theory, a method that is used to express the forces acting on a turbine.

Simplifications have to be made when simulating the circumstances near the installed prototype in an experiment with an open channel flume. These simplifications possibly lead to artifacts known as model effects and have for this case been described. Furthermore, four different flow conditions were selected that could best be tested in the planned experiments. The flow scaling parameters that have been considered in the design process of the model are the Froude and Reynolds number. The device scaling parameters that were taken into account are the scale factor, Tip Speed Ratio, thrust coefficient, torque coefficient and power coefficient.

The main conclusion of this work is that six scaling parameters need to be considered in the design of a physical scale model. Furthermore, it was concluded that a small scale factor and high free stream velocity in the model are favoured to minimize the scale effects for the Reynolds number. A limitation for the free stream velocity, however, is that the flow must remain sub-critical. Since Reynolds similarity is unlikely to be achieved in open channel flume experiments, it is recommended to adjust the pitch angle to approach similarity for the torque coefficient. If similarity for the Tip Speed Ratio and torque coefficient is reached, a correct ratio of kinetic power extraction from the flow is maintained in the model. Optimization of the model's design can best be done with experiments. This process will be an iterative process of adjusting the free stream velocity, angular velocity and pitch angle in the model.

Contents

List of Figures

List of Tables

1

Introduction

1.1. The Eastern Scheldt

Located in the Southwest of The Netherlands in the province of Zeeland lies the estuary the Eastern Scheldt (Figure 1.1). The Easten Scheldt *(in Dutch: De Oosterschelde)* is connected to the North Sea and surrounded by the peninsulas Schouwen-Duiveland, Tholen, Zuid-Beveland and Noord-Beveland. The estuary covers an area of approximately 350 km^2 and reaches about 48.1 km inland [10]. Nowadays, the Eastern Scheldt is separated from the North Sea by the Eastern Scheldt storm surge barrier.

Figure 1.1: Eastern Scheldt including floodplains from [1]

The North Sea flood of 1953, in which 1836 people died and almost 100,000 people had to be evacuated in The Netherlands, was the incentive for the Dutch government to revise the country's coastal defence plan [11]. In 1958 the parliament approved with the so called Delta Law that would prevent that a flood with the magnitude of 1953 could occur again. The idea behind the Deltaplan was to reduce the coastline length, so that it would be easier to defend the country against the sea [12]. The Deltaplan included the construction of the Eastern Scheldt storm surge barrier, the largest structure of the Dutch Delta Works.

The Eastern Scheldt barrier was build between 1976 and 1986 [2]. The barrier consists of 65 concrete pillars with 62 steel gates. The total length of the barrier (from Schouwen to Noord-Beveland) is 9 km of which 3 km is operable. At the sections Hammen, Schaar van Roggenplaat and Roompot the steel gates of the barrier can simultaneously and independently be opened or closed (Figure 1.2).

The Eastern Scheldt storm surge barrier was build to resist a water level that will statistically occur once in 4000 years. The barrier closes when a water level of +3.00 m NAP is expected. Under normal circumstances the steel gates are in open position, thereby allowing the Eastern Scheldt estuary to be influenced by the North Sea tide [12]. Since the tide in the Eastern Scheldt estuary is not identical to that at the North Sea, the water levels on both side of the barrier predominantly differ. This difference in hydraulic head can be a potential source for energy extraction by for example tidal stream turbines.

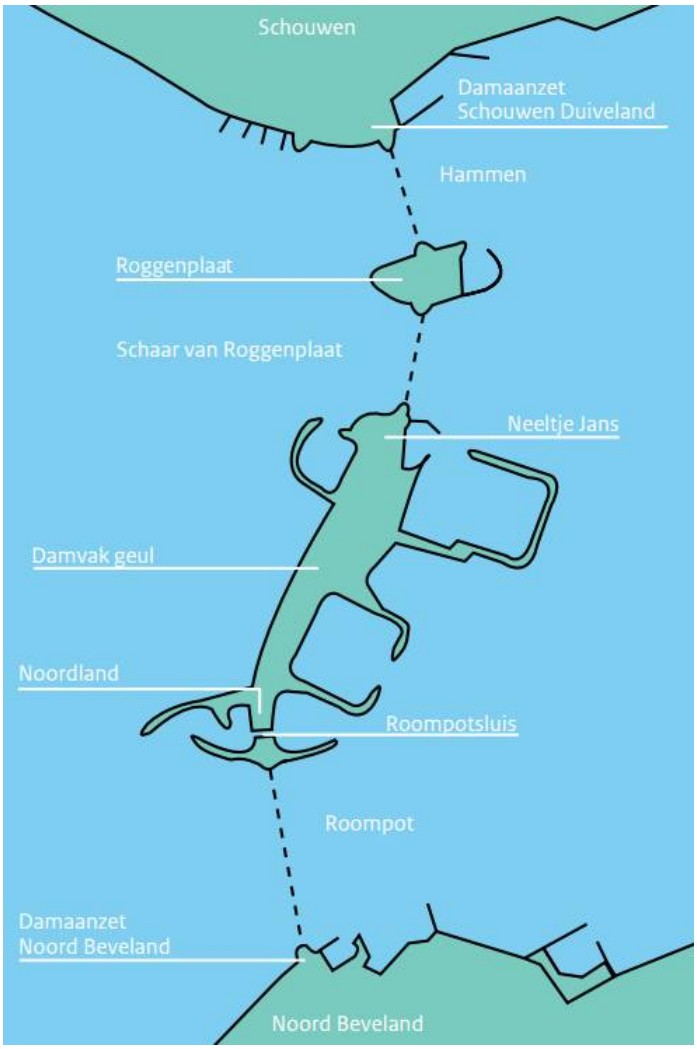

Figure 1.2: Schematic overview Eastern Scheldt storm surge barrier from [2]

1.2. Tidal Energy in the Eastern Scheldt

In order to transit to a more sustainable society the Dutch government has decided that 14 % of the national energy consumption in 2020 needs to come from renewable energy sources [13]. This share of green energy will further be increased to 16 % in 2023, as described in The Agreement on Energy for Sustainable Growth *(in Dutch: Het Energieakkoord)* of September 2016. In 2050 almost all the energy that the Dutch population consumes has to come from renewable energy sources [14]. The main sources in The Netherlands to produce this green energy are currently biomass, solar radiation and wind [15]. Another relatively new technology that is under development is the generation of energy from tidal currents. A tidal stream turbine uses a generator to convert kinetic energy from the fluid into electrical energy [16]. The technology of generating tidal energy is currently in the semi-commercial phase. The first large tidal stream farms are to date being build, e.g. the 398 MW Meygen project of Atlantis near the coast of Schotland [17].

In November 2015, the Dutch based company Tocardo International BV has installed five operating Horizontal Axis Tidal Turbines (HATT's) in the Eastern Scheldt storm surge barrier. These five two-bladed HATT's have a total capacity of 1.25 MW, and produce sufficient energy to provide the energy demand of 1000 households [3]. The HATT's are connected to a support structure that is installed between two concrete pillars in the barrier's Roompot section. The support structure makes it possible to lift the HATT's out of the water in case of large water level differences across the barrier or for maintenance and inspection. Furthermore, the HATT's function bi-directional, meaning that the turbines generate energy during in- and outflow of the estuary.

Figure 1.3: Tocardo's installed HATT's in the Eastern Scheldt storm surge barrier from [3]

Besides its primary purpose as sea defence it can thus be said that the Eastern Scheldt barrier is an attractive location for the generation of tidal energy. The maximum head loss over the barrier is approximately 1 m, corresponding to flow velocities in the barrier's gates of 4 m/s and higher [18]. The main advantage of generating energy from the flow through the Eastern Scheldt barrier is that the flow velocities are high and predictable. The phenomena causing the tidal flow, the gravitational pull of the sun and the moon and centrifugal forces of the Earth-Moon system, are well understood making tidal energy a reliable source [19].

Tocardo International BV has indicated that the company wants to expand the generation of tidal energy in the Eastern Scheldt. If up-scaling will be allowed, the technology to harness tidal energy will become more attractive as production costs decrease. However, before expansion of this form of energy generation can be considered, it should clearly be understood what the effects are on the Eastern Scheldt barrier and the environment. In a Green Deal between the province of Zeeland, the Dutch government and Tocardo, agreements were made that Tocardo could use the southwestern delta as testing location for their prototype, provided that the company would share the test results [3] [20].

A research group of the section Environmental Fluid Mechanics at Delft University of Technology is currently investigating the possible hydro-environmental effects of the installed HATT's in the Eastern Scheldt storm surge barrier. The interest of the research group goes out to the influence of upstream perturbations on the flow downstream of the HATT's. To investigate these effects experiments on a single downscaled turbine are planned in the summer of 2017. The experiments will be executed in an open channel flume of the Fluid Mechanics Laboratory at the TU Delft. The aim of the experiments is to gain a better understanding of the behavior of the wake, a hydraulic flow phenomenon that is observed directly downstream of a tidal stream turbine. Additionally, the performance of thrust and torque delivered by the turbine are aspects that will be considered during the planned experiments. A better understanding in these aspects will contribute to the knowledge if expansion of tidal energy generation in the Eastern Scheldt is to be advised.

1.3. Problem: Downscaling the Prototype to a Model

In order to investigate the influence of upstream perturbations on the installed prototype and the environment, a physical downscaled turbine model is required. This model will be used in experiments with an open channel flume at Delft University of Technology. To obtain useful results from these experiments, it is of importance that the model represents all physical properties of the prototype as good as possible. The following difficulties arise when downscaling Tocardo's installed prototype to a physical model:

1. *Model effects:* Since the situation near the Eastern Scheldt storm surge barrier is highly complex, it will be challenging to simultaneously downscale all physical properties such as the geometry of the structure, fluid characteristics, performance of the turbines, gravitational acceleration and atmospheric pressure [21]. It is likely that simplifications have to be made in order to downscale the prototype to a model.
2. *Scale effects:* Not all relevant prototype parameters can be scaled simultaneously such that they match with a downscaled model. Force ratio differences between the model and prototype will occur resulting in dissimilarity [21].
3. *Technical and financial trade-off:* The size at which the model will be reproduced will be a trade-off between the available budget and the desired accuracy. A full-scale model of the prototype will have the best corresponding test results, however at the expense of higher costs. In general, scale effects will tend to deviate more for an increasing scale factor [22] [23].
4. *Measurement effects:* It is likely that different measuring techniques will be used for collecting data from the model and prototype. Comparing data obtained from the model and prototype can therefore be misleading. It should be taken into account that each measuring technique has its own accuracy [21] [24].

All the above mentioned factors should be taken into account when downscaling the HATT's in the Eastern Scheldt barrier for experiments in the TU Delft laboratory. The designer will need to have knowledge of how the model is qualitatively and quantitatively affected by model effects, scale effects, technical and financial trade-off and measurement effects.

1.4. Objective and Research Question

The objective of this additional graduation work is to make recommendations for a feasible design of a downscaled physical model that strives to dynamic similarity with the installed Horizontal Axis Tidal Turbines by Tocardo International BV in the Eastern Scheldt storm surge barrier. Feasible refers to the ability to use the model in the open channel flume experiments at Delft University of Technology. Furthermore, all factors in this design that will cause dissimilarity between model and prototype will be considered.

The main research question of this report is:

What is the design of a physical model that best represents the properties of a Horizontal Axis Tidal Turbine in the Eastern Scheldt storm surge barrier, taking into account all the factors that cause model-prototype dissimilarity?

The following sub-questions are defined to answer the main research question:

1. What is the knowledge in literature about model-prototype similarity of Horizontal Axis Tidal Turbines?
2. What are the scaling parameters for the flow through the Eastern Scheldt storm surge barrier?
3. What are the scaling parameters for the turbine properties?
4. Which similarities are important with respect to the behavior of wake structures?
5. What dissimilarities arise when choosing certain scaling parameters?

1.5. Methodology

This additional graduation work can be characterized as a conceptual design study, in which recommendations are made for a physical scale model of the installed HATT's in the Eastern Scheldt barrier. The strategy used in this research can be explained in four steps (Figure 1.4).

The first step in the design process is to perform a literature review on what is currently known about the scaling of tidal stream turbines. In this step, insight will be gained into the parameters that are used to scale flow and turbine properties. Additionally, the results of studies that have investigated the near and far wake behavior downstream of scaled HATT's will be revised [25]. To get more understanding of all the force that are acting on a turbine, the literature review will end with an introduction of Blade Element Theory (BET).

In the second step, the scaling parameters for the flow and the turbine properties will be determined. Data of six Acoustic Doppler Current Profiler (ADCP) measurement devices that are mounted on the two outer and center turbine are for this research made available by Tocardo International BV. Furthermore, the company has shared torque and power data obtain from the aforementioned HATT's. Data of the water levels from measurement stations at the mouth of the estuary (seaward side barrier) and in the estuary are publicly accessible through the website of Rijkswaterstaat. The most important scaling parameters to be determined for the flow are the Froude number and the Reynolds number. For scaling the turbine the scale factor, Tip Speed Ratio (TSR), thrust coefficient, torque coefficients and power coefficient will be considered.

The third step will be to combine the scaling parameters for the flow and turbine properties and come up with a concept design for the physical model. If the student does not succeed to determined the required scaling parameters in the previous step, it will be stated what information or data is missing.

The last step is to assess the concept design by an analysis of the dissimilarities between the model and prototype. Adjustments to the design can be made in order to achieve better model-prototype similarity. In case that dissimilarities between model and prototype are so large that no useful results can be obtained in open channel flow experiments, the student will justify why no concept design for a physical model is feasible.

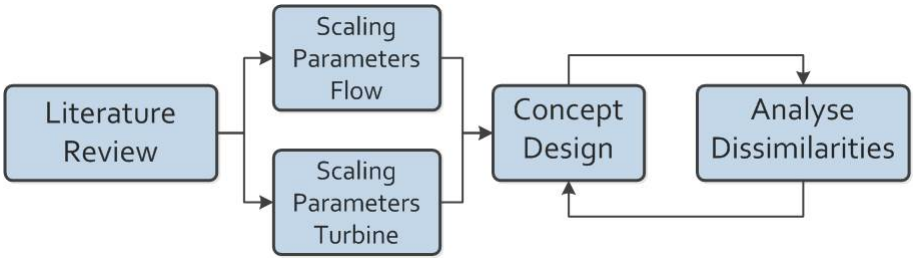

Figure 1.4: Schematic overview of the research strategy

1.6. Report Outline

This work consists of 4 chapters and an appendix A. In this first chapter an introduction was given of the Eastern Scheldt barrier and the potential it has to extract tidal energy by means of Tocardo's installed HATT's. Chapter 2 includes a literature review that informs the reader about the methods that can be used to scale HATT's. Additionally, previous studies that have investigate the wake structure downstream of tidal stream turbines will be discussed. The chapter ends with an short introduction of Blade Element Theory (BET). Chapter 3 focuses on the flow and device scaling parameters required to achieve model-prototype similarity. At last, chapter 4 states the main conclusions of this additional graduation work and mentions the recommendations for the planned experiments in the TU Delft water laboratory.

Appendix A includes an example of the Buckingham Pi Theorem, in which dimensionless numbers are formulated to scale the wake structure downstream of tidal stream turbines.

2

Literature Review

The purpose of this literature review is to discuss the different methods that can be used to achieve model-prototype similarity, and ascertain how these methods have been used in previous experiments. This chapter will first elaborate on the different types of similarities. Secondly, the different methods that are used to obtain similarity are explained. Thirdly, previous studies that have investigated the wake properties downstream of a downscaled tidal turbine or porous mesh disk will be discussed. The approaches and results of these experiments can help to set up the experiments that are planned in the laboratory at the TU Delft. At last, a short introduction of Blade Element Theory (BET) will be provide to inform the reader about the forces that act on a turbine.

2.1. Model-prototype Similarities

Different types of similarities between a model and prototype can be considered. Depending on the interests of the experiment a certain degree of similarity will be desired for the model. To achieve full model-prototype similarity, also refereed to as mechanical similarity, a model has to meet the following requirements:

1. *Geometric similarity:* A prototype and its physical model are geometrically similar if the ratios of all corresponding linear dimensions are equal [26]. This ratio is also known as the scale ratio or scale factor λ.

$$\lambda = \frac{L_p}{L_m} \tag{2.1}$$

   In Equation 2.1 L represents a characteristic length in the prototype and model, indicated respectively with subscripts p and m. Furthermore, it follows that areas and volumes of the prototype scale with a factor λ^2 and λ^3, respectively. Difficulties in geometric similarity can arise when the materials roughness is taken into account. Length scales of the prototypes roughness will become so small in a model, that it will be impractical to reproduce [27].

2. *Kinematic similarity:* A kinematic similar model requires similarity between the motion of particles in the model and prototype. In a geometric similar model, this results in the paths of all particles in the model to be identical to that of the prototype at all times [23].

3. *Dynamic similarity:* In addition to geometric and kinematic similarity, a dynamically similar model also requires that all force ratios between the model and prototype are identical. Important forces that should be considered in scaling hydraulic phenomena are the inertial force, gravitational force, viscous force, surface tension force, elastic compression force and pressure force [21].

As will be demonstrated later, it will be nearly impossible to scale all force ratios simultaneously in a model. As stated in [21]: "Exact model similarity would require a model operating in a *miniature universe* where all physical parameters are scaled including geometry, fluid properties, characteristics of the structure, gravitational acceleration and the atmospheric pressure." Models are therefore often scaled to the most relevant force ratio(s), with the awareness that scale effects are introduced.

2.2. Methods to obtain Similarity

Different methods can be used to investigate model-prototype similarity. The methods discussed in this section are the inspectional analysis, Buckingham Pi theorem, calibration and scale series.

2.2.1. Inspectional Analysis

In inspectional analysis the similarity between model and prototype is based on the equations by which the flow is described. The equations that govern the flow can be of a general form such as the Navier-Stokes equations, or more specified to the considered phenomenon. To apply this method the equations should include a balance between forces. In [28] the method of inspectional analysis is explained as follows. If the force balance in the prototype can be described by

$$A + B + C + ... = 0 \tag{2.2}$$

and an equivalent function can be formulated for the model

$$a + b + c + ... = 0 \tag{2.3}$$

then model-prototype similarity is obtained when the ratios between the individual contributions in the force balance are equal.

$$\frac{A}{a} = \frac{B}{b} = \frac{C}{c} = ... \tag{2.4}$$

In an inspectional analysis the formulated equations do not have to be solved for specific boundary conditions. The solution will finally need to obtained from the physical model [23].

Relevant forces in the field of fluid mechanics are the inertial force, gravitational force, viscous force, surface tension force, elastic compression force and the pressure force [23]. These forces result in the following five well known force ratios:

$$\text{Reynolds number:} \quad Re = \frac{UL\rho}{\mu} \tag{2.5}$$

$$\text{Froude number:} \quad Fr = \frac{U}{\sqrt{gL}} \tag{2.6}$$

$$\text{Cauchy number:} \quad Ca = \frac{K}{\rho U^2} \tag{2.7}$$

$$\text{Weber number:} \quad We = \frac{\rho L U^2}{\sigma} \tag{2.8}$$

$$\text{Euler number:} \quad Eu = \frac{p}{\rho U^2} \tag{2.9}$$

where the parameters indicate the flow velocity U, density of the fluid ρ, characteristic length L, dynamic viscosity μ, gravitational acceleration g, bulk modulus K, surface tension σ and pressure p. An extensive list of common force ratios is given by [29]. To obtain mechanical similarity all these force ratios need to be equal in the model and prototype [21].

The advantage of inspectional analysis is that insight is gained into the importance of the terms in the force balance. This, as in the next subsection will be explained, is not the case in a dimensional analysis where the relative influence of identified variables remains unknown. A second advantage is that due to the knowledge on the relative importance of terms, a minimum scale can be determined for which no large scale effects occur. A disadvantage of inspectional analysis, however, is that it can only be applied if equations are formulated that expressed the force balance. This requires profound knowledge of the considered hydraulic phenomenon [28] [21].

2.2.2. Buckingham Pi Theorem

The Buckingham Pi theorem [30] is a dimensional analysis that can be used to obtain similarity between a prototype and a physical model. An extensive explanation of the theorem can be found in [22]. In the theorem a certain hydraulic phenomenon described by n independent variables is written in the form of Equation 2.10. The exact function of f herein is not of importance.

$$f(q_1, q_2, ..., q_n) = 0 \tag{2.10}$$

The Buckingham Pi theorem states that if a phenomenon can be described by n independent variables $q_1, q_2, ..., q_n$ involving r basic dimensions, then (usually) $n-r$ dimensionless numbers $\Pi_1, \Pi_2, ..., \Pi_{n-r}$ can be formulated. In case of dynamic similarity, all dimensionless numbers that are formed should be equal in the model and prototype. The advantage of the theorem is that n independent variables can be reduced to $n - r$ dimensionless numbers. It results that Equation 2.10 can be rewritten as:

$$h(\Pi_1, \Pi_2, ..., \Pi_{n-r}) = 0 \tag{2.11}$$

A disadvantage of the Buckingham Pi theorem, however, is that the relative importance of the found dimensionless numbers remains unknown [21]. Furthermore, all independent variables should be identified by the user of the theorem when dynamic similarity is desired. If it is not possible to design a model such that all dimensionless numbers match between the model and prototype, a decision needs to be made for the most relevant force ratio. Insight into the considered phenomenon is then required [23]. An example of the application of the Buckingham Pi theorem can be found in Appendix A.

In the paper [31] by Mason-Jones et al. is described how a dimensional analysis can be used to reach model-prototype similarity for a tidal stream turbine. The key performance characteristics of tidal stream turbines are identified as the power, torque and thrust. It is shown how the power coefficient C_P, torque coefficient C_θ and thrust coefficient C_T are generated using the Buckingham Pi theorem,

$$C_P = \frac{P}{\frac{1}{2}\rho A_d U^3} \tag{2.12}$$

$$C_\theta = \frac{\tau}{\frac{1}{2}\rho A_d R U^2} \tag{2.13}$$

$$C_T = \frac{T}{\frac{1}{2}\rho U^2 A_d} \tag{2.14}$$

where P is the actual power output, A_d the rotor area, τ the torque, T the thrust and R the radius of the turbine. Furthermore, it is shown that the above mentionded turbine performance parameters are all functions of the Reynolds number and the Tip Speed Ratio (TSR). The Reynolds number and TSR are defined as, respectively,

$$Re = \frac{\rho U D}{\mu} \tag{2.15}$$

$$TSR = \frac{\omega R}{U} \tag{2.16}$$

where D is the diameter of the turbine and ω the angular velocity of the turbine blade. In the paper it is concluded that when Reynolds and TSR similarity is reached, the model and prototype have an equal turbine performance.

2.2.3. Calibration

Calibration is the oldest method used to achieve model-prototype similarity. It was first used by Sextus Julius Frontinus, who investigated the deposit of sand in Rome's aqueducts with a scale model [22]. In the method a physical scale model is calibrated such that it corresponds with the data measured in the prototype. This process is done by trial and error. If the parameters for which the physical model is scaled agree reasonably, then this gives confidence that the model will behave in a same way as the prototype for other testing configurations [21].

The disadvantage of calibration is that the method depends on the availability of data obtained from the prototype. The physical model can only be calibrated for the measured prototype scenarios. An advantage is that the researcher can adjust a large variety of parameters in the system, provided that the main effect is correctly reproduced in the model [22]. Furthermore, the method can still be an outcome if the considered phenomenon is too complex to formulate analytically, or too many variables are involved for a dimensional analysis [23].

2.2.4. Scale Series

In scale series several physical models with different scale factors are made of the prototype. The scaled models are then tested for similar conditions to investigate the influence of scale effects on the results. An advantage of this method is that scale effects can be quantified, or that it can be determined how the scale effects influence the test results. Additionally, the method can result in limiting criteria for which scale effects become significant. [21].

2.3. Previous Studies on Wake Structures

To date only a limited number of studies have investigated the near and far wake properties behind tidal stream turbines. An overview of these turbine wake studies until 2013 is given in [32]. The incentive for research mainly comes from the question how tidal stream turbines should be positioned in arrays. If tidal stream turbines become more commercially attractive, it is likely that the turbines are build in farms. The wake recovery length will especially then be of crucial importance for the performance of the turbines. Additionally, the effect that the wakes have on the environment is of interest. Previous studies include experiments with porous disks, mechanical rotors and Computational Fluid Dynamics (CFD) models. This section will discuss the results and conclusions from previous studies, and compared the different approaches used.

2.3.1. Mesh Disk Simulator

In [4] experiments have been done with mesh disks in a flume at the University of Southampthon Chilworth. The aim of the research is to identify the parameters that are involved in the formation of the wake structure downstream of a marine current turbine, and investigate the associated recovery length of the velocity profile.

According to the paper, the wake structure that is formed downstream of Marine Current Energy Converters (MCEC's) is caused by the flow velocity reduction of the fluid passing the plane of the rotor. The free stream velocity, which has not passed the rotor plane, still has a higher velocity. To conserve momentum the region with the reduced flow velocity needs to expand. This then forms a cone shaped structure, namely the wake. At the boundary layer the faster flowing free stream fluid re-energizes, breaks up and increases the velocity of the wake. Further downstream the flow in the wake recovers to the original velocity profile. The distance that the velocity profile needs to resume to its original shape is named the recovery length. In a previous paper [33] a distinction is made between the near and far wake. The near wake is characterized by the extraction of momentum from the flow, which results in an expansion of the wake structure. The driving force for the far wake structure is convection and turbulent mixing. In the experiments it is assumed that mesh disk simulators correctly reproduce the far wake properties.

In [4] it is stated that the of use physical turbine models or rotors becomes impractical for small scale experiments. It is shown with an example that a scaled rotor with a diameter of 100 mm would require to rotate above 1500 rpm to correctly scale flow properties, rotor thrust, power and tip speed. Since it is assumed that the thrust delivered by the MCEC's is of principal importance in the formation of the wake, use is made of porous disks to reproduce the energy extraction of the flow.

A disadvantage of the use of mesh disk simulators is that it does not result in the same effect on the flow as a rotor. The difference between a porous disk and a rotor lays in the following aspects:

1. A turbine extracts energy from the flow by mechanical motion. When a porous disks is used, energy is converted into small-scale turbulence.

2. The rotating blades of a turbine will have different vortexes sheds compared to that of a static porous disk.

3. A static mesh disk does not reproduce swirl, which will be present in the case of a rotor.

The important scaling parameters discussed in [4] to obtain similar flow conditions are the Froude and Reynolds number. The Froude number is of importance since the rotor is positioned close to the free surface. Gravitational effects can thus not be neglected in the system. Reynolds similarity should be maintained as, especially in the proximity of the seabed, viscous force cannot be neglected. The authors indicate that for small scale experiments difficulties can arise when both parameters are scaled simultaneously. For scaling hydraulic channel flows it is usually recommended to obtain the same Froude number in the model and prototype. It is then accepted for the Reynolds number to deviate, provided that the same turbulence classification is maintained. Furthermore, it is stated that the principal scaling parameter of the device is the trust coefficient C_T. The trust coefficient represents the ratio of the axial thrust force acting on the turbine to the kinetic energy available in the flow through the rotor plane, and quantifies the change in momentum by MCEC's.

From the results in [4] it can be concluded that for various trust coefficients the effect on the wake structure is limited in the region beyond 6 diameters downstream of the mesh disk. Another identified parameter that influences the wake structure is the distance between the mesh disk and the seabed. The results show that when the mesh disk is positioned closer to the seabed, the wake structure will expand further downstream. Lastly, the influence of bed roughness is discussed. A rougher seabed increases the amount of turbulence in the flow near the seabed. When the mesh disk is positioned in close proximity to seabed, the wake structure merges with the turbulent region near the bottom. This results in an expansion of the wake in downstream direction. When the mesh disk is located at a larger distance from the seabed, no significant deviations are observed from tests with a smooth seabed.

An example of how a wake structure can be visualized can be found in Figure 2.1. This figure shows the test results of experiment with 100 mm mesh disks. The mesh disks are positioned at two different depths in a open channel flume with added artificial bottom roughness. The mean flow velocity in this experiment is approximately 0.25 m/s. The parameter that is used to express and visualize the recovery of the velocity profile is the turbulence intensity I,

$$I \equiv \frac{u'}{\overline{U}} \tag{2.17}$$

where u' is the root mean square of the velocity fluctuations and $\overline{U}$ the mean flow velocity. Figure 2.1 shows that wake structures can be observed up to 20 diameters downstream of mesh disks.

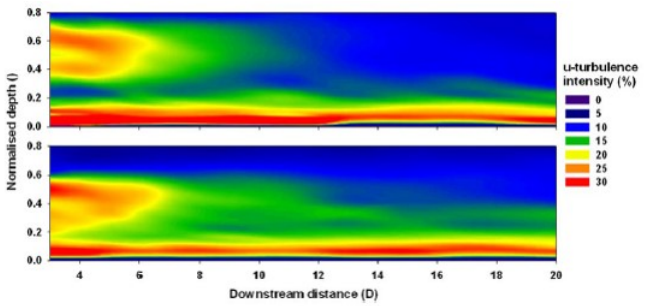

Figure 2.1: Centre plane turbulence intensity for two vertical positions of the mesh disk (top: 0.5d and bottom: 0.33d) from [4]

In the paper [25] the authors disagree with the use of mesh disk simulators to reproduce wake structure downstream of tidal stream turbines. According to Tedds et al., mesh disk simulators significantly overestimate the turbulent kinetic energy decay rate for modelled turbines.

Altogether, it will be doubtful if mesh disk simulators are suitable to correctly reproduce the wake structures that are observed downstream of tidal stream turbines. At the discretion of the author of this additional graduation work, a fundamental characteristic of tidal stream turbine is neglected when using mesh disks, namely the effect of rotation. The influence of swirl generated by the rotating turbine blades could be of significant importance in the persistence of the wake structure.

2.3.2. Physical Scaled Turbine Models

In [5] the results of experiments with a downscaled model of a tidal stream turbine are discussed. It is shown that the near wake region of HATT's is formed by the rotor and the influence of the turbine's support structure. Experiments with a 0.8 m diameter scaled turbine mounted on a circularly vertical tower, as depicted in Figure 2.2, have proven that the support structure significantly affects the wake structure that is formed downstream. Figure 2.3 depicts the results from tests with the rotor in a non-operational state to clearly show the effect of the support structure. In the experiment flow velocities of 0.8 m/s were maintained.

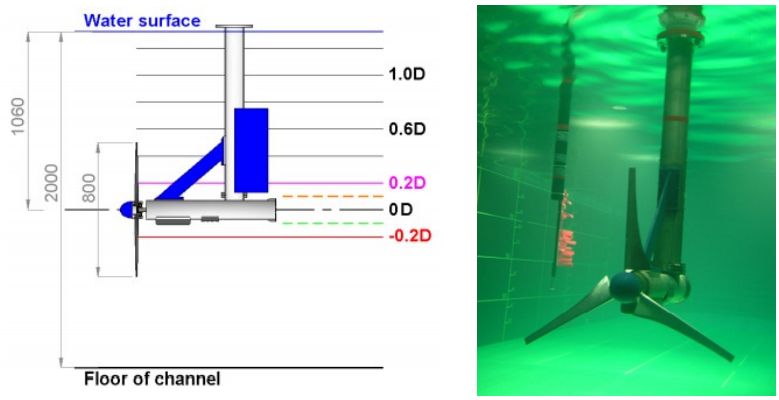

(a) Schematic overview model including relevant dimensions

(b) Impression of the physical model in the flume

Figure 2.2: Experiments investigating the importance of the support structure from [5]

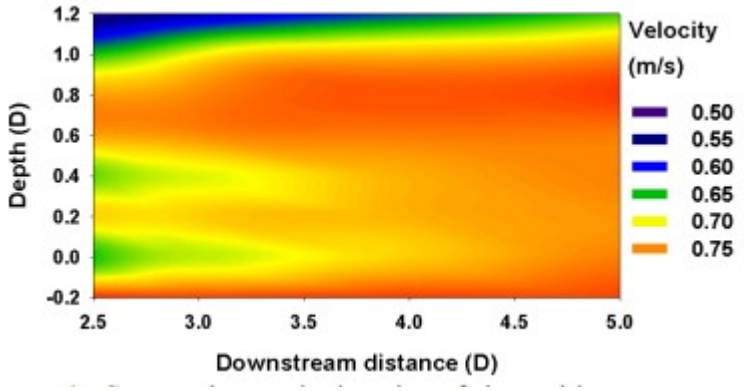

Figure 2.3: Centre plane velocity downstream a turbine support structure from [5]

In the results presented in Figure 2.3 the depth is scaled with the diameter of the turbine D with the hub located at $D = 0$. In this figure three regions can be observed with reduced flow velocities. The authors explain that the lowest region ($D = 0$) with a reduced flow velocity is caused by the trailing edge of the nacelle, the middle part ($D = 0.4$) due the flanges of the support tower and the upper region ($D = 1.2$) by the topside of the support structure. In conclusion, the paper states that the support structure has a significant influence on the formation of the near wake downstream of HATT's.

Research in [34] shows the influence of the quality of the incoming flow on the turbine performance and the wake structure. In experiments with a three-bladed 0.7 m diameter turbine the effect of increased ambient turbulence intensity has been investigated. The results show that for a higher ambient turbulence intensity the velocity profile and turbulent intensity return faster to their original shapes. From this paper can be concluded that it is of importance to correctly scale the ambient turbulence intensity in an experiment.

The influence of wake structures from nearby positioned tidal stream turbine is investigated in [35]. It was shown that the wakes of laterally positioned HATT's interact when the turbines are located in close proximity. Experiments were preformed with single and multiple 270 mm diameter rotors to compare the measured wake properties. It was found that for rotors with a lateral spacing (distance between the rotor centers) of three rotor diameters, the wake structures measured were comparable to that of a single rotor. However, when a lateral spacing of two rotor diameters or less is maintained the adjacent wakes start to merge. The paper also discusses the effect of irregular surface waves on the wake structure. In experiments, surface waves propagating in opposite direction to the flow velocity caused more than a doubling of the velocity fluctuations in the upper half of the wake structure. However, no significant changes were observed in the lateral and vertical profile.

In [16] experiments in a towing tank with 0.46 m diameter scaled HATT's have been executed. The advantage of experiments in a towing tank is that the influence of the flow velocity and surface waves can be tested simultaneously. In the paper it is concluded that surface waves affect the performance of a three-bladed turbine. However, it is not stated what the effect of surface waves is on the downstream wake of HATT's, and if this could possibly be tested in a towing tank.

From experiments with physical scaled turbine models was learned that several aspects are important to consider when setting up an experiment to reproduce wake structures. Factors that should be taken into account in the design process are the support structure, ambient turbulence intensity, lateral spacing between the turbines and surface waves. Since it will impracticable to simultaneously simulated all these aspects in a single experiments with an open channel flume, a decision must be made for the most relevant factors.

2.3.3. Computational Fluid Dynamics Models

Additional research to near and far wake structures downstream of mesh disks and HATT's has been done with CFD models. Studies as [36], [37] and [38] have shown that CFD models are capable of producing similar test results as obtained from physical experiments. These type of models can thus be used with confidence.

The results of wake studies by CFD models will not be discussed here. For further information on the research done with CFD models the reader is referred to a selection of papers stated in Table 2.1.

Author	Year	Reference
Li et al.	2017	[38]
Blackmore et al.	2014	[39]
Batten et al.	2013	[36]
Harrison et al.	2010	[37]
Harrison et al.	2009	[40]
Sun et al.	2007	[41]
Bryden et al.	2002	[42]

Table 2.1: Overview of CFD studies on tidal stream turbine wake structures

2.4. Blade Element Theory

Blade Element Theory (BET) is used as a method to optimize the design of wind turbines. In this theory the blade of a turbine is subdivided into several small elements. For each of these elements the forces are then determined. With BET it is possible to formulate expressions for the power, thrust and torque.

The theory is to a large extent also applicable to marine turbines. An important difference, however, is that marine turbines can be exposed to cavitation [43]. A concise explanation of BET for a wind turbine is given in [6].

To derive expressions for the total thrust force F_T and torque T_r acting on a turbine, a blade element at constant length r from the rotation axis is considered. This blade element is subject to an axial wind speed V and a rotational speed of the blade element $r\Omega_r$. As a first approximation, the relative wind speed V_{rel} can be derived from those two components. The blade element experiences two forces, namely a lift force f_L and a drag force f_D. The lift force acts in perpendicular direction to the relative wind speed, while the drag force acts in the same direction. Furthermore, these forces can be resolved into an axial force f_T and a tangential force f_r. A schematic overview of the relative wind speed and forces acting on a blade element is shown in Figure 2.4.

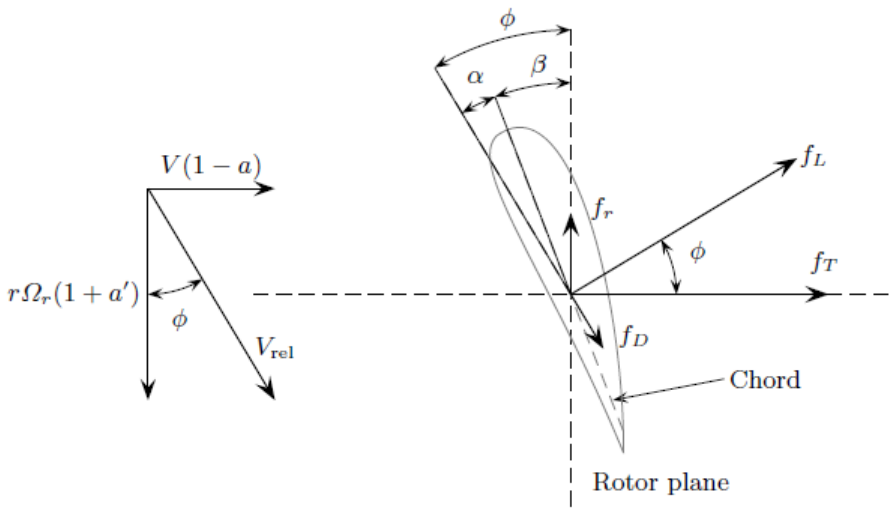

Figure 2.4: Schematic overview of the forces acting on a blade element from [6]

In the above figure α represents the incident angle (angle between the relative wind speed and the chord) and β the pitch angle (angle between the chord and the rotor plane). Furthermore, ϕ is defined as the sum of α and β. In the left scheme of Figure 2.4 $(1-a)$ and $(1+a')$ indicate the correction factors for the relative wind speed. For more information on these factors is referred to [6].

The lift force and drag force per unit length are expressed as follows:

$$f_L = \frac{\rho c}{2} V_{rel}^2 C_L(\alpha) \tag{2.18}$$

$$f_D = \frac{\rho c}{2} V_{rel}^2 C_D(\alpha) \tag{2.19}$$

where c is the chord length of the considered blade element, C_L the lift coefficient and C_D the drag coefficient. As can be seen in the above formulas, the lift and drag coefficient are both functions of the incident angle. An important indicator for the performance of a wind turbine is the ratio C_L/C_D. High values of this ratio are favourable in the design of wind turbines, since it expresses the amount of useful torque generated. It should be noted that for a high angle of attack a sudden drop of the ratio C_L/C_D occurs ($\alpha \cong 13°$ for aerofoils). This state is know as stall and significantly affects the efficiency of turbines.

Using the angles as defined in Figure 2.4 the axial force and torque τ_r per unit length can be formulated as:

$$f_T = \frac{\rho c}{2} V_{rel}^2 (C_L(\phi-\beta)cos(\phi) + C_D(\phi-\beta)sin(\phi)) \tag{2.20}$$

$$\tau_r = \frac{\rho c}{2} V_{rel}^2 r(C_L(\phi - \beta)sin(\phi) - C_D(\phi - \beta)cos(\phi)) \tag{2.21}$$

Two important relations can be derived from the Equation 2.20 and Equation 2.21. The total axial thrust force is determined by contributions from the lift and drag forces. On the other hand, useful torque is only developed by the lift force, since the drag force acts in the opposite direction (Figure 2.5).

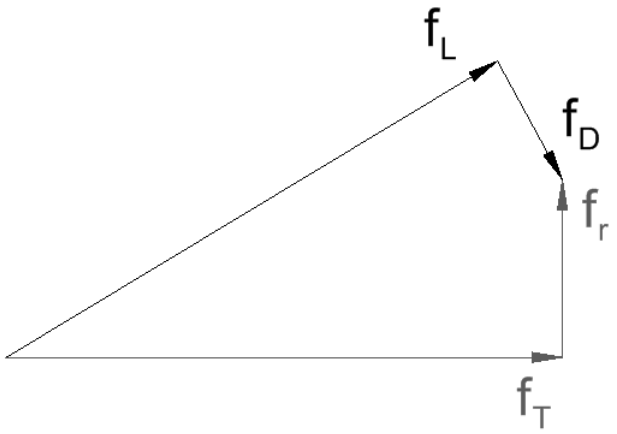

Figure 2.5: Contributions to axial and tangential forces

Integration of Equation 2.20 and Equation 2.21 along the entire blade length results in the total thrust force and torque acting on the rotor:

$$F_T = \frac{1}{2}\rho\pi R^2 C_T(TSR, \beta)V^2 \tag{2.22}$$

$$T_r = \frac{1}{2}\rho\pi R^3 C_\theta(TSR, \beta)V^2 \tag{2.23}$$

where R is the radius of the turbine blade. Subsequently, the power P_r can be derived with the following expression:

$$P_r = \frac{1}{2}\rho\pi R^2 C_P(TSR, \beta)V^3 \tag{2.24}$$

The thrust, torque and power coefficients are all dependent on the TSR and the pitch angle. Since the example in [6] explains the scenario of a wind turbine, the TSR is given by:

$$TSR = \frac{R\Omega_r}{V} \tag{2.25}$$

in which Ω_r is the angular velocity of the turbine blade.

In the remainder of this section two papers will be discussed that are related to the theory discussed above. It is shown that the angle of attack and the Reynolds number can significantly affect the drag and lift coefficients.

In order to investigate the efficiency of hydro-kinetic turbine blade profiles a numerical performance analysis was applied on various pre-developed blade sections [7]. In this study the program JavaFoil was used to determine the lift, drag and pressure coefficients of RISO, NREL and NACA hydrofoils. Results of the calculated C_L/C_D ratios for the hydrofoils are shown in Figure 2.6. Depending on the type of hydrofoil, the maximum values of C_L/C_D are expected to occur for angles of attack between 4 till 8 degrees.

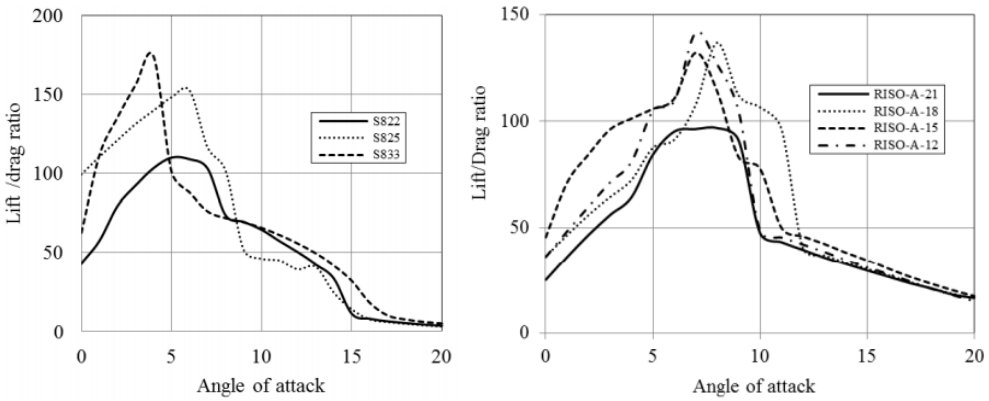

(a) NREL (b) RISO

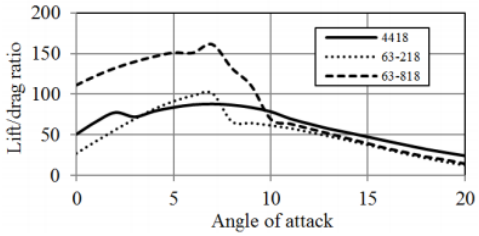

(c) NACA

Figure 2.6: C_L/C_D ratios for various types of hydrofoils ($Re = 1 \times 10^6$) from [7]

In [8] is described how the Reynolds number affects the lift and drag coefficients of an aerofoil. Figure 2.7 shows the drag and lift coefficient of the NACA0012 aerofoil for different Reynolds numbers. It can be seen that for increasing values of the Reynolds number the drag coefficient decreases. In contrast to the drag coefficient, the lift coefficient increases with higher Reynolds numbers.

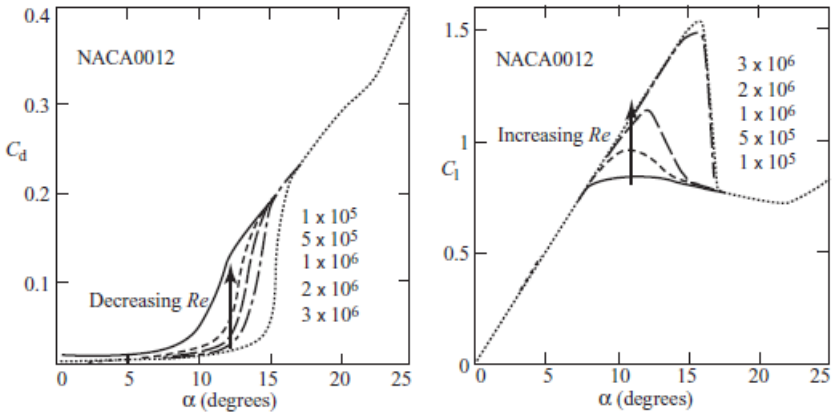

Figure 2.7: Lift and drag coefficients of an aerofoil for different Reynolds numbers from [8]

2.5. Summary/Discussion Literature

This literature study reveals that several types of similarities can be reached between a physical model and prototype. For the planned experiments in the TU Delft water laboratory dynamic similarity is desired, since force ratios play an important role in correctly scaling wake structures. However, to achieve dynamic similarity between a model and prototype all force ratios will need to be scaled simultaneously. Since this is nearly impossible, a decision must be made for the most relevant scaling parameter in wake structures.

Several scaling methods have been discussed that could be used to scale Tocardo's installed turbines in the Eastern Scheldt storm surge barrier to a physical model. The ability to use the inspectional analysis, Buckingham Pi theorem, calibration or scale series depends on the knowledge of the considered phenomenon and the data available from the prototype. Since no analytical expressions can be formulated that express the force balance of wake structures, the inspectional analysis cannot be applied to scale the wake structure downstream of Tocardo's turbines. Scaling laws therefore have to be formulated by means of a dimensional analysis, in which the relative importance for the found dimensionless parameters remains unknown.

Although the literature on wake structures downstream of tidal stream turbines to date is limited, several factors have been identified from previous studies that influence wake structure downstream of HATT's. Experiments have shown the effects of the thrust, vertical position of the turbine, bed roughness, support structure, ambient turbulence, nearby turbine wakes and surface waves on the formation of wake structures. All these factors are important to consider when scaling Tocardo's turbines in the Eastern Scheldt. It is highly questionable, however, if all these factors can simultaneously be taken into account in a single experiment.

Previous research on wake structures with mesh disk simulators and turbine models often only considers the results of the experiments, and scarcely state what scaling methods or laws were used to obtain model-prototype similarity. Additionally, a lack of knowledge in literature comes from experiments performed with two-bladed HATT's. The discussed experiments in this literature review were all performed with mesh disks simulators or three-bladed turbine models. The effects of wakes downstream of two-bladed HATT's is therefore still unknown. Advantage of two bladed turbines over three bladed turbines is that productions costs are less, and that the total weight of the turbine decreases due the amount of blades. A disadvantage of a two bladed turbine, however, is that it has to rotate faster in order to have the same efficiency as a three bladed turbine [44].

At last, a short introduction is given of Blade Element Theory. It has been explained how the lift and drag forces contribute to the thrust force and torque acting on the rotor. Furthermore, research results have been discussed that show the influence of the angle of attack on the ratio C_L/C_D, and the effect of the Reynolds number on the lift and drag coefficients.

Since a wide range of dimensionless numbers can be obtain when applying a dimensionless analysis to the considered situation in the Eastern Scheldt, a decision has to made for the most relevant scaling parameters. In this report six scaling parameters will be considered to correctly scale the prototype to a physical scale model. The first scaling parameter that will be considered is the scale factor. Geometric similarity of the physical scale model is achieve when all dimensions of the prototype are scaled with a constant scale factor. The second scaling parameter is the Tip Speed Ratio. Equal values for this scaling parameter in the prototype and model will result in kinematic similarity. Lastly, to approach dynamic similarity the Froude number, Reynolds number, thrust coefficient, torque coefficient and power coefficient are taken into account.

The Cauchy number and Weber number are in this study not considered as important scaling parameters. The elastic force and surface tension force are not expected to significantly affect the wake structure downstream of tidal stream turbines and are therefore not considered.

3

Design Physical Scale Model

The aim in the design process of the physical scale model of the Tocardo's Eastern Scheldt turbines is to maintain equal scaling parameters between the model and prototype. To achieve this the current situation is first simplified such that the conditions in the prototype can be simulated in an experiment with an open channel flume. Then, the flow conditions are determined that will be reproduced in these experiments. The selected scaling parameters in the literature review will in this chapter be divided into two categories: flow scaling parameters and device scaling parameters. The flow scaling parameters are considered as the Froude and Reynolds number. Additionally, the device scaling parameters that will be treated are the scale factor, Tip Speed Ratio (TSR), thrust coefficient, torque coefficient and power coefficient. At last, the scale effects will be discussed that affect the results of experiments with a scaled turbine model.

3.1. Simplification of the Current Situation

The area of interest of the Eastern Scheldt storm surge barrier can be characterized as complex as various factors influence the flow through the structure, and thus affect the performance of the installed tidal stream turbines. Figure 3.1 gives an impression of the streamlines computed by Deltares with a CFD model in the proximity of the gate with the installed HATT's. In the figure can be seen that the incoming streamlines from the North Sea are straight and parallel during flood. Due to a decreasing bottom level and the geometry of the of the Eastern Scheldt barrier the streamlines contract near the gate. This contraction of streamlines results in an increase of the flow velocity, which in the figure is indicated by the color bar. Downstream of the gate the influence of the tidal stream turbines and the deceleration of the flow can clearly be observed from the more chaotic streamlines. With an increasing distance downstream from the turbines, the streamlines become straighter again. Also, it can be seen that due to an increasing depth the flow velocities decrease to their original state.

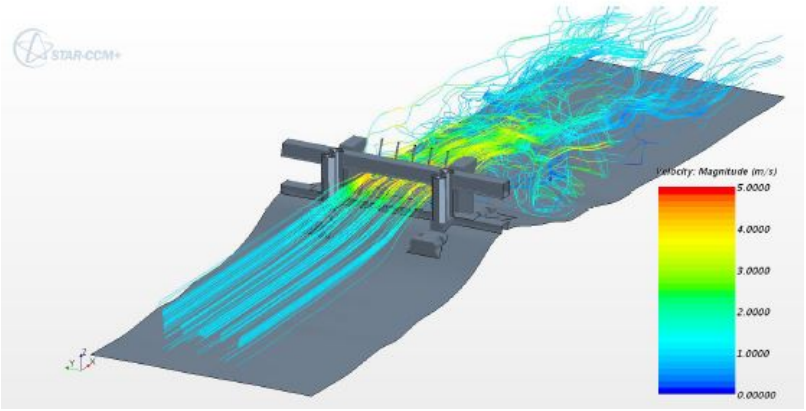

Figure 3.1: Streamlines through the Eastern Scheldt barrier with tidal stream turbines from [9]

The current situation near the installed HATT's will be simplified in the planned experiments, to isolate the processes that influence the wake structure. These simplifications introduce model effects and cause experimental reveals to differ from observations in the prototype. In the next paragraph an attempt will be made to qualitatively describe the simplifications and the effects they have on the outcomes of the experiments.

The simplifications involve that the experiments will be executed in an open channel flume with a horizontal flat bottom instead of a seabed with a varying bottom topography. To simulated the flow acceleration near the gate, which in the prototype is caused by the varying bottom depth and the geometry of the barrier, use in the experiments will be made of a spillway. This simplification implies that in the experiment the flow is only constricted in the vertical direction and not, as in the case of the prototype, also in the horizontal direction. Another simplification is that the experiments will be executed with only one scaled turbine model. This is a significant simplification as the HATT's in the prototype are placed in close proximity of each other such that the downstream individual wakes merge into a large wake structure. In the experiments the effect of merging wakes will thus not be included. The last simplification is the absence of bed protection in the experiments. The seabed protection near the Eastern Scheldt barrier mainly consist of block mats, rock dump and asphalts mastic [45]. This seabed protection will result in an increase of turbulence near the bottom boundary. An option to compensate for this increased turbulence in the experiments is to add artificial roughness to the flume's bottom plate.

The simplifications finally lead to an experimental setup in an open channel flume as depicted in Figure 3.2. It should be noted that the figure is not to scale, and that the dimensions of the presented spillway can be altered to obtain the desired contraction.

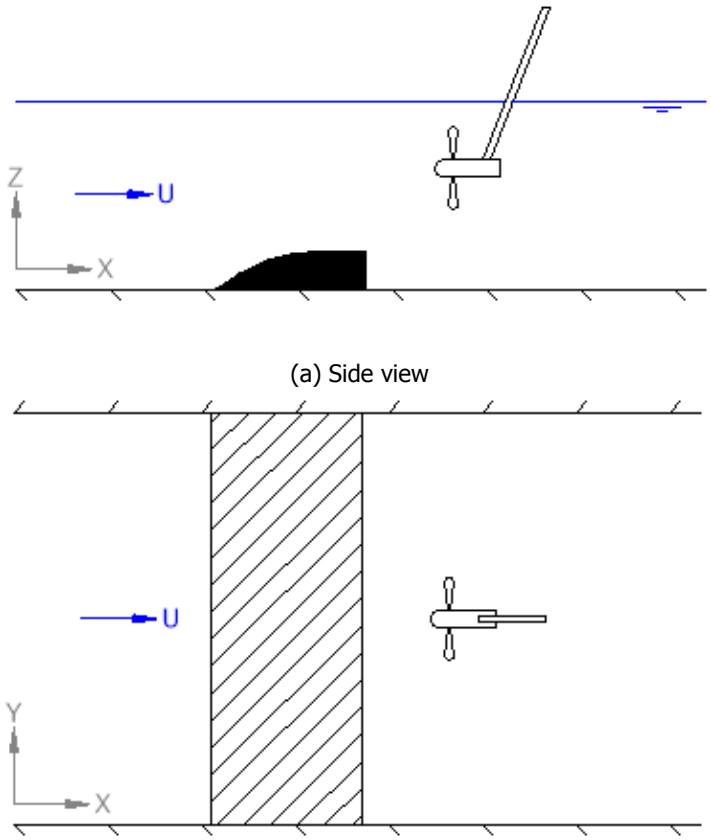

(a) Side view

(b) Top view

Figure 3.2: Schematic overview setup experiment TU Delft open channel flume

Since the financial budget for the planned experiments is limited, the physical model cannot be build at the full scale of the prototype. To reduce costs the physical model is reduced in size such that the experiments can be executed in a open channel flume of the TU Delft water laboratory. For the planned experiments two open channel flumes are available. The dimensions of these flumes including the maximum recommended diameter for the physical scale model are stated in Table 3.1.

	Length [m]	Width [m]	Max. depth [m]	Diameter model [mm]	Scale factor [-]
Flume 1	9.50	0.50	0.65	100	52.7
Flume 2	39.00	0.80	0.85	160	32.9

Table 3.1: Dimensions of the available flumes in the TU Delft laboratory with associated physical models

The maximum diameter of the physical scale model is based on the width of the flume. Due to friction the flow velocity reduces near the lateral boundaries of the flume, resulting in a non-uniform horizontal velocity profile. To make sure that this effect does not influence the outcomes of the experiments, sufficient spacing is required between the scaled model and the lateral boundaries. In previous experiments with scaled tidal turbine models, no open channel flumes were used with a width less than 5 diameters of the scaled turbine model. This will therefore be the starting point for the dimensions of physical scale models. In the remainder of this report a comparison will be made between the 100 mm and 160 mm diameter model, referred to as Model 1 and Model 2 respectively.

3.2. Different Conditions: Spring and Neap Tide

The amount of energy that can be extracted by Tocardo's turbines from the flow through the Eastern Scheldt barrier is dependent on the flow velocities through the gate. This flow velocity varies over time due to the tide at the North Sea. During spring tide the water level difference is maximum resulting in the greatest potential for energy extraction. For neap tide the maximum water level difference is minimum and energy extraction will be less attractive. Figure 3.3 depicts the water level difference Δh determined from data measured at tide stations Roompot Buiten and Roompotbinnen for October 2016. The tide stations Roompot Buiten and Roompot Binnen are located approximately 3 km seaward of the barrier and near the barrier in the estuary, respectively. The water level data was obtained from the website of Rijkswaterstaat.

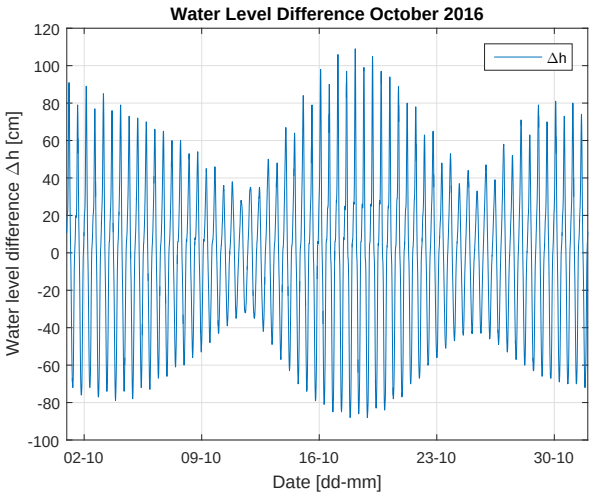

Figure 3.3: Water level difference Roompot Buiten and Roompot Binnen

For the planned experiments in the TU Delft water laboratory it would be interesting to simulated the flow conditions of the neap and spring tide. The maximum flow velocities through the gate per tidal cycle are determined by these two events. Figure 3.4 shows the water levels measured at Roompot Buiten and Roompot Binnen during spring and neap tide in October 2016. From these graphs the

exact times can be determined for which the flow velocities are maximum. Additionally, the effect of the direction of the flow could be of interest in experiments. Since the HATT's are installed on the estuary side of the barrier, flow conditions differ significantly during ebb and flood. In total four flow conditions are advised to be simulated in the planned experiments, namely the spring and neap tide scenarios during both ebb and flood.

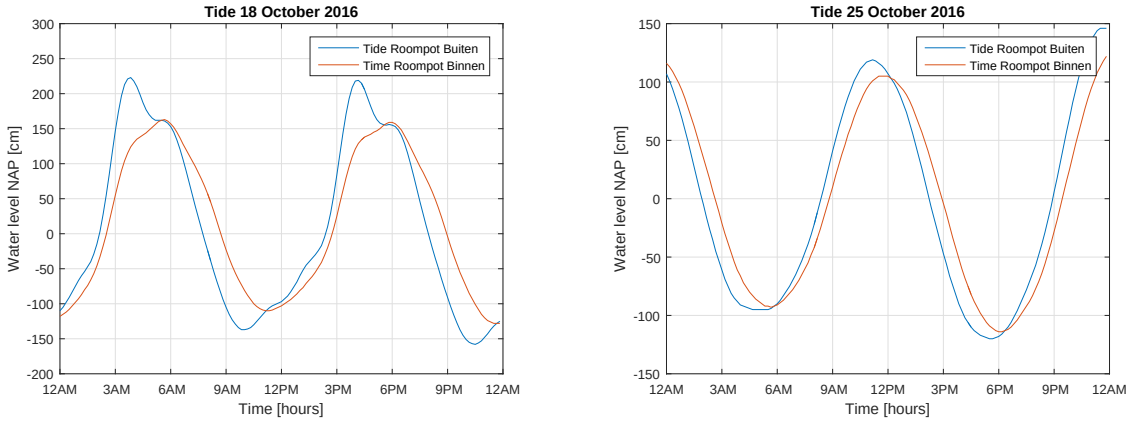

(a) Spring tide

(b) Neap tide

Figure 3.4: Water levels during spring and neap tide for Roompot Binnen and Roompot Buiten

3.3. Flow Velocity Profile

Since the installation of the Tocordo turbines in the Eastern Scheldt barrier, data is continuously being collected to monitor the performance of the prototype. Tocardo International BV has made this data available for the currently ongoing research at the TU Delft. The collected data includes the measured flow velocity, power, and Rotations Per Minute (RPM) of the two outer and middle turbine from October 10, 2016 to October 25, 2016. The flow velocity per turbine is measured by two ADCP measurement devices oriented in seaward and landward direction.

Figure 3.5 indicates the absolute values of the measured flow velocity during neap and spring tide, in which the positive horizontal position is chosen in the direction of the Eastern Scheldt. Each data point represents the averaged flow velocity of 1 minute sampling. The blue bars indicate the standard deviation measured during this time interval. Matlab was used to plot a 9^{th} degree polynomial fitting curve through the data points. It should be noted that during spring tide the turbines are lifted out of the water due to restrictions imposed by Rijkswaterstaat. In the event of spring tide the turbines are only operational approximately half of the time. No data is therefore available for the extreme flow conditions during spring tide. Flow conditions for spring tide (flood and ebb) that will be simulated in the experiments are determined by the points in time that the turbines are still operational (Figure 3.5a and Figure 3.5b).

A few remarks can be made when observing the data presented in Figure 3.5:

1. Missing flow velocity data: At the location of the turbine (horizontal position $2-5$m) the flow velocity is not measured. This can be explained by the positions of the ADCP's on the turbine.

2. Higher flow velocity on the seaward side: The flow velocities are relatively higher, since the velocity is measured in the gate where the flow is contracting.

3. Larger deviation downstream: Due to a higher turbulence intensity downstream of the turbine the horizontal velocity shows a larger deviation from the mean velocity.

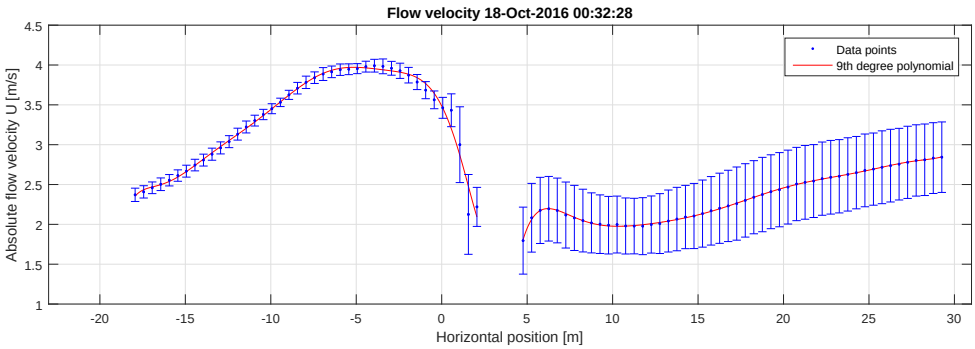

(a) Spring tide: flood (flow from left to right)

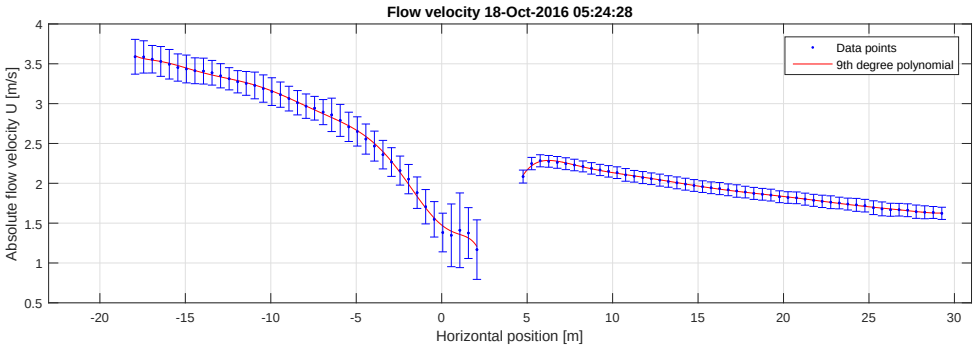

(b) Spring tide: ebb (flow from right to to)

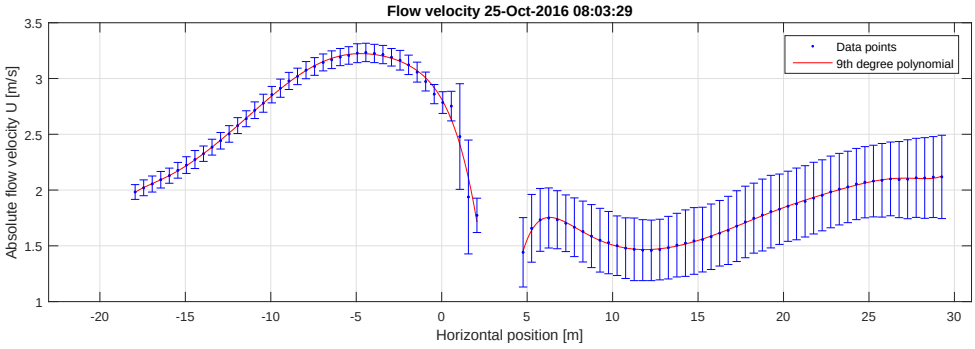

(c) Neap tide: flood (flow from left to right)

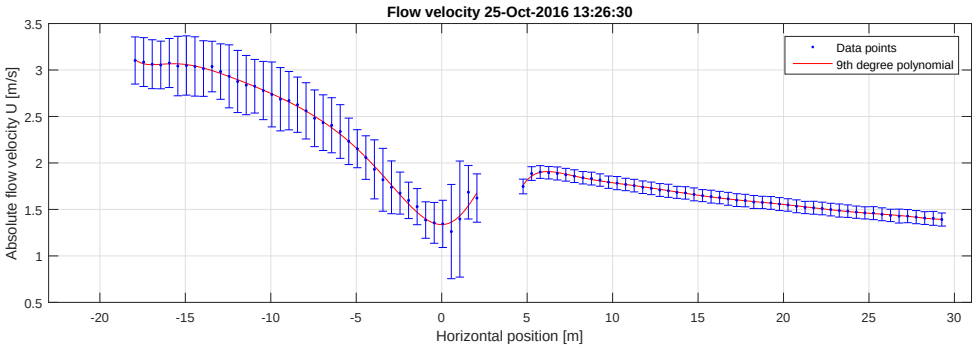

(d) Neap tide: ebb (flow from right to left)

Figure 3.5: Maximum flow conditions during spring and neap tide

3.4. Flow Scaling Parameters

As identified in the literature review, two important dimensionless numbers used to scale the flow are the Froude number and Reynolds number. This section will discuss both parameters and inform the reader on the values that can be expected in experiments.

3.4.1. Froude Number

The Froude number expresses the ratio of the inertia force over the gravitational force. Especially in cases where a free stream flow is induced by a gravitational force, Froude similarity should be considered [46]. Figure 3.6a depicts the Froude number in the prototype and scale models for different characteristic flow velocities. To compute the Froude number the diameter of the turbine was chosen as the characteristic length. It can be seen that when Froude similarity is maintained, the characteristic flow velocities in the open channel flumes do not exceed 1 m/s. The Froude number will however not be the most relevant scaling parameter for scaling the flow, since surface waves are not expected to have a dominant influence on the wake structure downstream of tidal stream turbines.

3.4.2. Reynolds Number

The second dimensionless parameter that is considered to scale the flow is the Reynolds numbers. The Reynolds number expresses the ratio of the inertial force over the viscous force. The Reynolds number could be favourable as the principle scaling parameter in hydraulic phenomenon, such as the wake structures downstream of tidal turbines, where viscous forces play a dominant role. The disadvantage of Reynolds similarity, however, is that for down-scaled turbine models the flow velocity increases relatively to the prototype. As can be seen in Figure 3.6b, the flow velocities required to achieve Reynolds similarity are beyond the limitations of the available open channel flumes. The maximum flow velocities feasible in the flumes of the TU Delft water laboratory are in the order of 1 m/s. The Reynolds numbers in the graph are based on the radius of the turbine as characteristic length. Additionally, different values were used for the dynamic viscosity in the prototype and models. The open channel experiments will most likely be executed with fresh water at room temperature, while the prototype is situated in salt water and a colder environment. For experiments in an open channel flume this results in a relatively lower dynamic viscosity and thus higher Reynolds number.

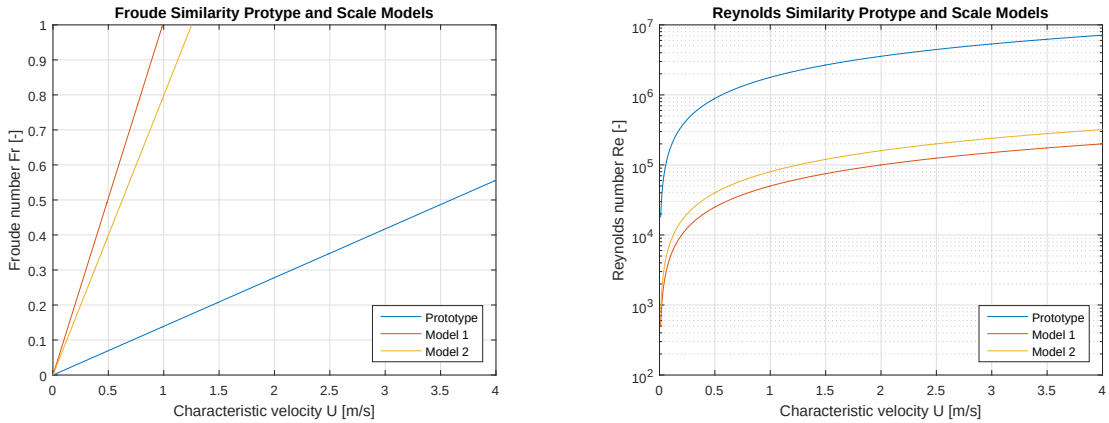

(a) Froude number similarity

(b) Reynolds number similarity

Figure 3.6: Froude and Reynolds similarity for prototype and scale models

3.4.3. Quantification of the Flow Scaling Parameters

The remaining unknown parameter to determine the exact values for the Froude number and Reynolds number in the prototype is the characteristic flow velocity U_{char}. As shown in Figure 3.5 the flow velocity differs per scenario and distance from the turbine. In this work the characteristic flow velocity is chosen as the incoming flow velocity measured at the largest distance from the ADCP measurement device. During flood the characteristic flow velocity is thus determined on the North Sea side of the

barrier and during ebb on the Eastern Scheldt side. Table 3.2 summarizes the found values for the characteristic flow velocities including the Froude and Reynolds numbers per flow condition. In order to correctly scale the flow in the model, it is sufficient to maintain the same order of magnitude of the Froude number and Renolds number as in the prototype.

		Characteristic flow velocity [m/s]	Froude number [-]	Reynolds number [-]
Spring tide	flood	$+2.355$	0.33	4.19×10^6
	ebb	-1.628	0.23	2.89×10^6
Neap tide	flood	$+1.980$	0.28	3.52×10^6
	ebb	-1.396	0.19	2.48×10^6

Table 3.2: Froude and Reynolds numbers in the prototype for different flow conditions

As can be seen from Figure 3.6b Reynolds similarity between model and prototype cannot be achieved in experiments with an open channel flume. Due to limitations of the flow velocities in experiments, the Reynolds number will be smaller in the model. To minimize the scale effects for the Reynolds number, the free stream velocity in be model needs to be set as high as possible. A restricting criteria, however, is that the flow must remain sub-critical ($Fr < 1$ based on the water depth). It follows that the model will, at all times, have a higher Froude number and a lower Reynolds number compared to the prototype. As an example, a free stream velocity in the model of 1 m/s results in a Froude number of approximately 0.9 and a Reynolds number around 4.5×10^4.

It should be noted that in the literature the characteristic velocity is often taken as the undisturbed incoming flow velocity. The ADCP devices mounted on the turbine do not measure this undisturbed flow velocity. From Figure 3.5 can be seen that no constant velocities are being measured at the largest distance upstream of the turbine. The flow within the reach of the ADCP devices are thus affected by the varying bottom depth and Eastern Scheldt barrier and cannot be classified as undisturbed. As a first approach, the measured disturbed flow velocity will satisfy to make quantitative approximations. However, it should to be taken into account that the undisturbed flow velocities will be lower, and that this will affect all scaling parameters that are a function of the characteristic flow velocity.

3.5. Device Scaling Parameters

The device scaling parameters that will be considered in the design of the physical scale model are the scale factor, Tip Speed Ratio (TSR), thrust coefficient, torque coefficient and the power coefficient.

3.5.1. Geometric Design

The geometric design of the physical scale model is completely determined by the decision for the scale factor (Equation 2.1). As discussed in section 2.1, the scale factor of the model will be based on the width of the available open channel flumes. For flume 1 and flume 2 this results is scale models with a turbine diameter of 100 mm and 160 mm, respectively. Furthermore, all other corresponding linear dimensions of the model and prototype will be scaled with this scale factor. Small details such as bolts and measurement instruments can be exclude from the geometric design, since these are of a negligible length scale compared to the dimensions of the turbine.

3.5.2. Tip Speed Ratio

The second device scaling parameter that will be considered is the TSR (Equation 2.16). The TSR expresses the ratio of the blade's tip speed over the velocity of the flow. In order to determine the TSR per flow condition, the angular velocity ω is computed from the measured RPM (Equation 3.1). The positive and negative values of the RPM and angular velocity indicate the direction of rotation. Table 3.3 summarizes the calculated TSR per scenario. The TSR's during ebb are smaller than the values for flood due to the decision for the characteristic flow velocity as incoming velocity.

$$\omega = \frac{2\pi \times \text{RPM}}{60} \tag{3.1}$$

		Characteristic flow velocity [m/s]	RPM [-]	Angular velocity [rad/s]	TSR [-]
Spring tide	flood	+2.355	+45.11	+4.72	5.29
	ebb	−1.628	−40.67	−4.26	6.89
Neap tide	flood	+1.980	+41.87	+4.38	5.84
	ebb	−1.396	−34.94	−3.66	6.91

Table 3.3: TSR in the prototype for different flow conditions

To indicate what rotational speeds can be expected in the experiments, the required RPM values for Model 1 and Model 2 are, for spring tide (flood) and neap tide (ebb), stated in Table 3.4. To calculate the RPM a free stream velocity in the flumes of 1 m/s was assumed. The computed values for the rotational speed are high, however, can be obtained in experiments. It can be concluded that the larger Model 1 operates at a significantly lower rotational speed to achieve kinematic similarity.

	TSR [-]	RPM Model 1 [-]	RPM Model 1 [-]
Spring tide flood	5.29	631.4	1010.3
Neap tide ebb	6.91	824.8	1319.7

Table 3.4: Rotational speeds of Model 1 and Model 2 for different flow conditions

3.5.3. Thrust Coefficient

In order to achieve model-prototype similarity the thrust coefficients in the model must be equal to the prototype (Equation 3.2). The indices p and m indicate the parameters in the prototype and model respectively.

$$C_{T,p} = C_{T,m} \tag{3.2}$$

As was explained in the literature review, the thrust coefficient is a function of the TSR, pitch angle and Reynolds number. If these parameters are equal in model and prototype, similarity of the thrust coefficient is also achieved. Unfortunately, Reynolds similarity cannot be achieved in the experiments since values are expected to be lower. As explained in section 2.4, a decreased Reynolds number results in a smaller lift coefficient and larger drag coefficient. The lift and drag force per unit length will therefore decrease and increase, respectively. Depending on the individual contributions of the lift and drag forces, the model's axial force f_T will increase, decrease or remain the same. The effect on the total thrust force and thrust coefficient of the model will therefore remain unknown (Equation 2.14). In literature values of $C_{T,m} \approx 0.9$ are commonly used [25].

Figure 3.7 depicts how an original force balance, indicated in black, can be affect by a decreased Reynolds number. The force balances in blue and red both show solutions for an increased drag force and a decreased lift force per unit length. In comparison, the force balance indicated in blue results in a decrease of the total thrust force, while the force balance in red results in an increased value.

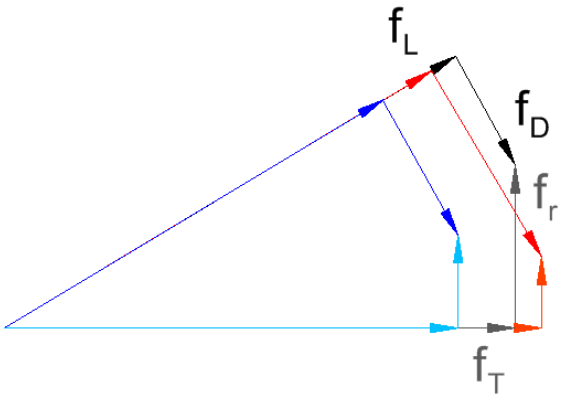

Figure 3.7: Effects of a decreased Reynolds number on the force balance of a blade element

3.5.4. Torque Coefficient

The fourth device scaling parameter that will be considered in this design is the torque coefficient. Once more, to obtain model-prototype similarity both coefficients must be equal in the prototype and model (Equation 3.3).

$$C_{\theta,p} = C_{\theta,m} \tag{3.3}$$

Similar to the thrust coefficient, the torque coefficient is also a function of the TSR, pitch angle and Reynolds number. Due the effect of a decreased Reynolds number in the model, the model's tangential force per unit length f_r will with certainty decrease (Figure 3.7). This results in a smaller torque per unit length and thus a decrease of the total developed torque. In conclusion, a decreased Reynolds number in the model will cause the model's torque coefficient to be smaller than that of the prototype.

To compensate the effect of the decreased Reynolds number, the pitch angle in the model can be adjusted such that higher values of the ratio C_L/C_D are obtained. A higher value of this ratio will increase the amount of useful torque and thus the model's torque coefficient. As discussed in section 2.4, maximum value of the ratio C_L/C_D for hydrofoils occurs around angles of attack of 4 till 8 degrees. CFD results in [31] have shown that values for the torque coefficient up to 0.14 can be expected in experiments.

3.5.5. Power Coefficient

The following relation between the torque coefficient, power coefficient and the TSR is given in [6]:

$$C_\theta = \frac{C_P}{TSR} \tag{3.4}$$

From the expression it can be concluded that if similarity for the torque coefficient and TSR between the model and prototype is achieved, this inevitably results in similarity of the power coefficient (Equation 3.5). Similarity of the power coefficient implies that the same ratio of power output to the kinetic power available in the flow through the rotor swept area, is maintained between the model and prototype [31]. In literature maximum values of the power coefficient of approximately 0.45 are found [47] [31].

$$C_{P,p} = C_{P,m} \tag{3.5}$$

3.6. Scale Effects

Scale effects result from the difference in scaling parameters between the model and prototype. This section will separately discuss the scale effects for to the flow and device scaling parameters. Finally, a strategy will be proposed to achieve the smallest scale effects in experiments.

3.6.1. Froude and Reynolds Dissimilarity

The scale effects for the flow scaling parameters directly follow from the decision that is made for the scale factor and free stream velocity. As discussed in subsection 3.4.3, experiments with the available flumes will both result in a larger Froude number and smaller Reynolds number compared to the prototype. A larger Froude number in the model results in an underestimation the gravitational force with respect to the inertial force. Furthermore, a too small Reynolds number implies that the viscous force is overestimated with respect to the inertial force. Lastly, from Figure 3.6 it can be concluded that a small scale factor is favourable to minimize the scale effects of the flow parameters.

3.6.2. Dissimilarities due to Device Scaling Parameters

Scale effects in the geometric design arise when small elements in the prototype are not included in the physical scale model. It could be that some elements, for example bolts, become too small to reproduce in the model. It is however not expected that these elements will significantly influence the outcomes of the experiments. Another scale effect in the geometric design of the model arises when the pitch angle is adjusted.

Unfortunately, with the current data it is not possible to quantify the thrust and torque coefficients of the prototype, and thus the magnitude of the scale effects caused by these scaling parameter. Thrust and torque data measured at the turbines is currently available, however, how this data should be interpreted remains unknown by the author of this work. If the prototype's thrust and torque coefficients would be known, then the prototype's thrust and torque coefficients can be determined. Subsequently, the magnitude of the corresponding scale effects remain a function of the model's free stream velocity, total thrust force and torque acting on the scaled turbine. The latter two parameters are difficult to compute and can best be measured during the experiments.

A strategy to achieve the smallest scale effects for the device scaling parameters would be to consider the TSR and torque coefficient as principal scaling parameters. This strategy would contain the following steps:

1. Make a decision for the scale factor of the physical scale model. This decision will be based on the dimensions of the available flume.
2. Preset the free stream velocity of the flume. The decision for the free stream velocity can be based on the magnitude of the scale effects for the Froude and Reynolds number.
3. Adjust the angular velocity of the model to obtain equal TSR between the model and prototype. This can for example be done by regulating of a mechanic or magnetic break.
4. Measure the thrust force and torque acting on the model and determine the model's thrust and torque coefficients.
5. Alter the pitch angle of the turbine blades to adjust the lift and drag forces such that the torque coefficients between the model and prototype deviate less.
6. Repeat step 3 till 5 to optimize the model's torque coefficient.

If similarity for the TSR and torque coefficient is accomplished, then it follows that the power coefficients for the model and prototype will also be equal. This implies that the correct amount of kinetic power is extracted from the flow. The magnitude of the scale effect for the thrust coefficient can be determined by the measurements of the total thrust force acting on the physical scale model. A schematic overview of the above strategy is depicted in Figure 3.8.

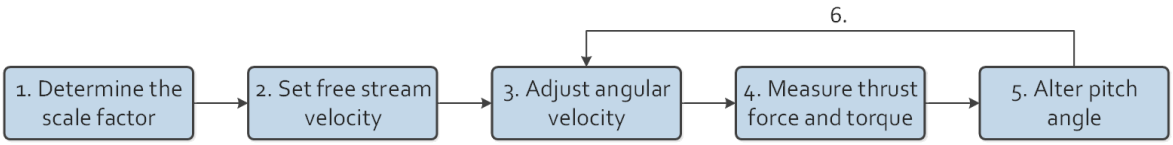

Figure 3.8: Schematic overview reduction strategy scale effects

4

Conclusions and Recommendations

4.1. Conclusions

This additional graduation work has investigated the design parameters for a physical downscaled model of the by Tocardo International BV installed turbines in the Eastern Scheldt storm surge barrier. Recommendations have been made that strive to dynamic similarity between the prototype and a proposed scale model that will be used in experiments with an open channel flume at the TU Delft. The main research question of this additional graduation work was:

What is the design of a physical model that best represents the properties of a Horizontal Axis Tidal Turbine in the Eastern Scheldt storm surge barrier, taking into account all the factors that cause model-prototype dissimilarity?

In the literature review was shown that different types of similarities can be achieved. In order to obtain useful results in experiments with a downscaled physical model, dynamic similarity is favoured between the prototype and model. In addition to geometric and kinematic similarity, dynamic similarity requires that all force ratios between model and prototype are equal. Furthermore, several studies have been discussed that mention important factors in scaling Horizontal Axis Tidal Turbines for research on wake structures. Factors that were identified are the effects of the thrust, vertical position of the turbine, bed roughness, support structure, ambient turbulence, nearby wake structures and surface waves.

In total six scaling parameters have been considered in the design of a physical scale model. These scale parameters are divided into flow and device scaling parameters. The flow scaling parameters in the prototype were successfully determined for different flow conditions. For all scenarios the flow is characterized as sub-critical, since Froude numbers vary between $0.19 - 0.33$. Furthermore, Reynolds numbers were found in the order of 1×10^6 which indicate fully turbulent flow. The only device scaling parameter that could be quantified was the Tip Speed Ratio. Unfortunately, insufficient data was available to determine the thrust and torque coefficients of the prototype.

A concept design for a physical downscaled turbine model that best represents Tocardo's Eastern Scheldt turbines is dependent on the dimensions of the flume that will be used in the experiments. The scale factor of the physical scale model can be based on the width of flume, to ensure that effects of the lateral boundaries are negligible. A small scale factor is favourable, since this decreases the scale effects for the Froude and Reynolds number.

To correctly scale the wake structure in the model, the Reynolds number is preferred as principal flow scaling parameter. However, it was shown that it is not feasible to achieve Reynolds similarity in experiments with an open channel flume. Reynolds numbers in the model will at all times remain smaller than that of the prototype. To minimize the scale effect of the Reynolds number it is recommended to increase the free stream velocity in the experiment, provided that the flow remains sub-critical ($Fr < 1$).

A consequence of maintaining a smaller Reynolds number in the experiment is that it affects the lift and drag forces acting on the turbine blades. Using Blade Element Theory it was shown that the tangential force per unit length decreases. This results in a decrease of the total torque developed by the physical model, and thus a smaller torque coefficient in the model. To compensate for the decreased torque coefficient, the model's pitch angle can be altered such that the ratio C_L/C_D increases. An increase of this ratio will result in more useful torque and thus increase the model's torque coefficient again. To what extend the pitch angle needs to be adjusted, and how this will affect the model's thrust coefficient remains unknown and can best be determined in experiments.

Scale effects in the model arise since not all scaling parameters can simultaneously be maintained in the model and prototype. The magnitude of scale effects for the flow parameters is determined by the decision for the scale factor and the model's free stream velocity. The magnitude of the scale effects for the device parameters can be quantified by means of experiments, provided that additional thrust and torque data from the prototype is made available. At last, this work has proposed a strategy to further optimize the scale model by considering the Tip Speed Ratio and torque coefficients as principal device scaling parameters.

4.2. Recommendations Experiment TU Delft Water Laboratory

Recommendations for the planned experiments in the water laboratory of TU Delft follow from the literature review and the considered scaling parameters.

- Research in [4] has shown that the vertical position of the scale model influences the wake structure downstream. It is therefore recommended to position the turbine at relatively the same water depth as in the prototype.
- Additionally, in [4] the influence of bottom friction was discussed. The bottom plates of the flumes in the TU Delft water laboratory consist of glass. It would be more realistic to add extra bed roughness in the experiments to simulate the presence of bed protection near the Eastern Scheldt barrier. This could for example be reproduced by applying sandpaper to the flume's bottom plate.
- As was shown in [5] the support structure of the model significantly affects the flow downstream of the turbine. Remarkable in Tocardo's design is that the support structure is positioned at an angle with the vertical. It is advised to include this support structure in the geometric design of the scale model, since this will most likely affect the wake structure downstream of the turbine.
- In [34] the effect of ambient turbulence intensity on the wake structure was demonstrated. It is recommended to determine the turbulence intensities in the prototype for the different flow conditions and maintain these values in the experiments. The turbulence intensity of the incoming flow in the model can be adjusted by means of honeycombs flow straighteners.
- It is advised to exclude surface waves, since this significantly complicates the setup of the experiment.
- It is recommended to maintain small angles of attack in the experiments. For angles of attack larger than $\alpha \cong 13^\circ$ (for aerofoils) stall occurs, causing a sudden drop in the C_L/C_D ratio [8]. From Figure 2.6 it can be seen that depending on the type of hydrofoil considered, stall occurs at smaller angles of attack compared to aerofoils.
- It is advised to use the Tip Speed Ratio and torque coefficient as principal scaling parameters to approach dynamic similarity between the physical scale model and the prototype. If similarity for these parameters is achieved, then it follows that the power coefficient between prototype and model is also equal.
- The scale effects for the flow are determined by the scale factor and the free stream velocity. It is recommended to use the larger flume 2 for the planned experiments, since this will reduce the scale effects for the Froude and Reynolds number.

A

Buckingham Pi Theorem Applied

The Buckingham Pi theorem can be used to gain insight into the parameters that are of importance to scale the wake properties downstream of the prototype to a physical model. It is assumed that the wake downstream of the tidal stream turbine is a function f of the flow velocity U $[LT^{-1}]$, density of the water ρ $[ML^{-3}]$, turbine diameter D $[L]$, dynamic viscosity μ $[ML^{-1}T^{-1}]$, angular velocity ω $[T^{-1}]$, gravitational acceleration g $[LT^{-2}]$, bulk modulus K $[ML^{-1}T^{-2}]$ and thrust T $[MLT^{-2}]$.

$$f(U, \rho, D, \mu, \omega, g, K, T) = 0 \tag{A.1}$$

As mentioned in subsection 2.2.2, the exact function of f is not of importance. Figure A.1 depicts a schematic overview of the identified independent variables in a wake structure downstream of a tidal stream turbines.

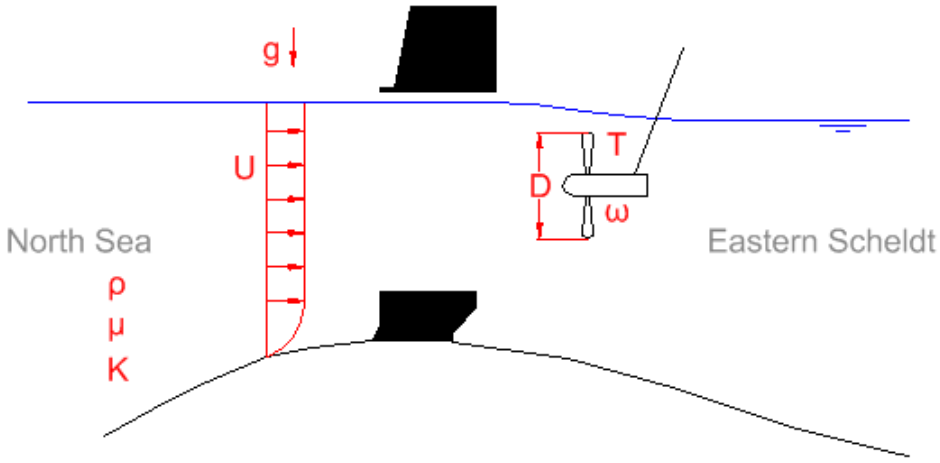

Figure A.1: Schematic overview variables Buckingham Pi theorem

Indicated in the square brackets the eight independent parameters $(n = 8)$ are expressed in the basic dimensions $r = 3$ of mass [M], length [L] and time [T]. From these independent parameters $n - r = 5$ independent dimensionless parameters $\Pi_1, \Pi_2, ..., \Pi_5$ can be formulated. Equation A.1 can thus be simplified to a function h of five dimensionless numbers.

$$h(\Pi_1, \Pi_2, ..., \Pi_5) = 0 \tag{A.2}$$

The flow velocity U, density ρ and diameter turbine D are chosen as repeating variables, since they contain all the basic dimensions and do not form dimensionless number by themselves. An expression for the first dimensionless parameter can now be given as:

$$\Pi_1 = U^a \rho^b D^c \mu \tag{A.3}$$

To solve the unknown exponents a, b and c, the repeating parameters will be replaced by their dimensions.

$$[-] = [LT^{-1}]^a [ML^{-3}]^b [L]^c [ML^{-1}T^{-1}] \tag{A.4}$$

The parameter Π_1 is dimensionless and thus Equation A.4 can be rewritten to a set of three equations including three unknowns.

$$\begin{aligned} [L]: \quad & 0 = +1a - 3b + 1c - 1 \\ [T]: \quad & 0 = -1a + 0b + 0c - 1 \\ [M]: \quad & 0 = +0a + 1b + 0c + 1 \end{aligned} \tag{A.5}$$

Or in matrix form:

$$\begin{bmatrix} 0 \\ 0 \\ 0 \end{bmatrix} = \begin{bmatrix} 1 & -3 & 1 \\ -1 & 0 & 0 \\ 0 & 1 & 0 \end{bmatrix} \begin{bmatrix} a \\ b \\ c \end{bmatrix} + \begin{bmatrix} -1 \\ -1 \\ 1 \end{bmatrix} \tag{A.6}$$

Solving the above set of equations result is: $a = -1$, $b = -1$, and $c = -1$. Substitution in Equation A.3 gives the final expression for the first dimensionless number.

$$\Pi_1 = \frac{\mu}{UD\rho} \tag{A.7}$$

The same can be done for the other four dimensionless parameters. The calculation of the exponents is done in the same way as displayed above. The expressions for the remaining dimensionless numbers are given below:

$$\Pi_2 = \frac{D\omega}{U} \tag{A.8}$$

$$\Pi_3 = \frac{gD}{U^2} \tag{A.9}$$

$$\Pi_4 = \frac{K}{\rho U^2} \tag{A.10}$$

$$\Pi_5 = \frac{T}{\rho D^2 U^2} \tag{A.11}$$

The wake downstream of a tidal stream turbine can now be described by a function h that is only depending on five dimensionless numbers.

$$h\left(\frac{\mu}{UD\rho}, \frac{D\omega}{U}, \frac{gD}{U^2}, \frac{K}{\rho U^2}, \frac{T}{\rho D^2 U^2}\right) = 0 \tag{A.12}$$

When some modifications are made to the found dimensionless numbers, it can be seen that expressions correspond with to the aforementioned force ratios in subsection 2.2.1. Changing the nominator and denominator of the found expressions is allowed since they are dimensionless.

Bibliography

[1] Wikipedia, *North sea flood of 1953,* (2010).

[2] Rijkswaterstaat, *Oosterscheldekering,* (Unknown).

[3] Tocardo, *Tidal power plant in dutch delta works,* (Unknown).

[4] L. Myers and A. Bahaj, *Experimental analysis of the flow field around horizontal axis tidal turbines by use of scale mesh disk rotor simulators,* Ocean Engineering **37**, 218 (2010).

[5] L. Myers and A. Bahaj, *Near wake properties of horizontal axis marine current turbines,* in *Proceedings of the 8th European Wave and Tidal Energy Conference* (Uppsala, Sweden, 2009) pp. 558–565.

[6] F. D. Bianchi, R. J. Mantz, and H. De Battista, *The Wind and Wind Turbines* (Springer, 2007).

[7] A. Muratoglu and M. I. Yuce, *Performance analysis of hydrokinetic turbine blade sections,* Journal ISSN **2** (2015).

[8] T. Burton, D. Sharpe, N. Jenkins, and E. Bossanyi, *Wind energy handbook* (John Wiley & Sons, 2001).

[9] DMCE, *Demand driven research & development,* (2017).

[10] P. H. Nienhuis and A. Smaal, *The Oosterschelde Estuary (The Netherlands): A case-study of a changing ecosystem*, Vol. 97 (Springer Science & Business Media, 2012).

[11] Y. Visser, *Watersnoodramp (1953) – een rampzalige stormvloed,* (2013).

[12] K. Steenepoorte, *De stormvloedkering*, Tech. Rep. (Rijkswaterstaat, 2016).

[13] Rijksoverheid, *Rijksoverheid stimuleert duurzame energie,* (Unknown).

[14] Unknown, *The Agreement on Energy for Sustainable Growth: a policy in practice*, Tech. Rep. (Sociaal-Economische Raad (Social and Economic Council), 2013).

[15] CBS, *Hernieuwbare elektriciteit; productie en vermogen,* (2017).

[16] L. Luznik, K. A. Flack, E. E. Lust, and K. Taylor, *The effect of surface waves on the performance characteristics of a model tidal turbine,* Renewable energy **58**, 108 (2013).

[17] Atlantis, *Meygen,* (Unknown).

[18] A. Bijlsma, A. Tralli, W. Verbruggen, and P. De Haas, *Detailed hydrodynamics of the eastern scheldt storm surge barrier: validation of a cdf approach,* 4th International Symposium of Shallow Flows (2017).

[19] F. O. Rourke, F. Boyle, and A. Reynolds, *Tidal energy update 2009,* Applied Energy **87**, 398 (2010).

[20] Rijksoverheid, *Green deal van provincie zeeland met de rijksoverheid,* (Unknown).

[21] V. Heller, *Scale effects in physical hydraulic engineering models,* Journal of Hydraulic Research **49**, 293 (2011).

[22] P. Novák and J. Cabelka, *Models in hydraulic engineering; physical principles and design applications* (Pitman Advanced Publishing Program, 1981).

[23] S. A. Hughes, *Physical models and laboratory techniques in coastal engineering*, Vol. 7 (World Scientific, 1993).

[24] T. Pullen, N. Allsop, C. Bruce, A. Kortenhaus, H. Schüttrumpf, and J. Van der Meer, *Wave Overtopping of Sea Defences and Related Structures: Assessment Manual*, Tech. Rep. (EurOtop, 2007).

[25] S. Tedds, I. Owen, and R. Poole, *Near-wake characteristics of a model horizontal axis tidal stream turbine,* Renewable Energy **63**, 222 (2014).

[26] J. Warnock, *Hydraulic similitude,* Engineering hydraulics (1950).

[27] D. Vassalos, *Physical modelling and similitude of marine structures,* Ocean engineering **26**, 111 (1998).

[28] D. M. Hanes and B. Le Méhauté, *Ocean engineering science*, Vol. 9 (Harvard University Press, 2005).

[29] R. Ettema, R. Arndt, P. Roberts, and T. Wahl, *Hydraulic modeling: Concepts and practice* (American Society of Civil Engineers, 2000).

[30] E. Buckingham, *On physically similar systems; illustrations of the use of dimensional equations,* Physical review **4**, 345 (1914).

[31] A. Mason-Jones, D. O'doherty, C. Morris, T. O'doherty, C. Byrne, P. Prickett, R. Grosvenor, I. Owen, S. Tedds, and R. Poole, *Non-dimensional scaling of tidal stream turbines,* Energy **44**, 820 (2012).

[32] S. Tedds, *Scale model testing of tidal stream turbines: wake characterisation in realistic flow conditions*, Ph.D. thesis, University of Liverpool (2014).

[33] A. Bahaj, L. Myers, M. Thomson, and N. Jorge, *Characterising the wake of horizontal axis marine current turbines,* in *Proceedings of the 7th European wave and tidal energy conference* (2007) p. 9.

[34] F. Maganga, G. Germain, J. King, G. Pinon, and E. Rivoalen, *Experimental characterisation of flow effects on marine current turbine behaviour and on its wake properties,* IET Renewable Power Generation **4**, 498 (2010).

[35] T. Stallard, R. Collings, T. Feng, and J. Whelan, *Interactions between tidal turbine wakes: experimental study of a group of three-bladed rotors,* Phil. Trans. R. Soc. A **371**, 20120159 (2013).

[36] W. M. Batten, M. Harrison, and A. Bahaj, *Accuracy of the actuator disc-rans approach for predicting the performance and wake of tidal turbines,* Phil. Trans. R. Soc. A **371**, 20120293 (2013).

[37] M. Harrison, W. Batten, L. Myers, and A. Bahaj, *Comparison between cfd simulations and experiments for predicting the far wake of horizontal axis tidal turbines,* IET Renewable Power Generation **4**, 613 (2010).

[38] X. Li, M. Li, S. J. McLelland, L.-B. Jordan, L. O. Amoudry, R. Ramirez-Mendoza, and P. D. Thorne, *Modelling tidal stream turbines in a three-dimensional wave-current fully coupled oceanographic model,* Renewable Energy (2017).

[39] T. Blackmore, W. Batten, and A. Bahaj, *Influence of turbulence on the wake of a marine current turbine simulator,* in *Proc. R. Soc. A*, Vol. 470 (The Royal Society, 2014) p. 20140331.

[40] M. Harrison, W. Batten, and A. Bahaj, *A blade element actuator disc approach applied to tidal stream turbines,* in *OCEANS 2010* (IEEE, 2010) pp. 1–8.

[41] X. Sun, J. Chick, and I. Bryden, *Laboratory-scale simulation of energy extraction from tidal currents,* Renewable Energy **33**, 1267 (2008).

[42] A. MacLeod, S. Barnes, K. Rados, and I. Bryden, *Wake effects in tidal current turbine farms,* in *International conference on marine renewable energy-conference proceedings* (2002) pp. 49–53.

[43] A. Molland, A. Bahaj, J. Chaplin, and W. Batten, *Measurements and predictions of forces, pressures and cavitation on 2-d sections suitable for marine current turbines,* Proceedings of the Institution of Mechanical Engineers, Part M: Journal of Engineering for the Maritime Environment **218**, 127 (2004).

[44] Unknown, *Turbine topologies: Number of blades,* (2008).

[45] J. Van Noortwijk and H. Klatter, *Optimal inspection decisions for the block mats of the eastern-scheldt barrier,* Reliability Engineering & System Safety **65**, 203 (1999).

[46] J. Battjes, *Vloeistof Mechanica* (Delft University of Technology, 2002).

[47] L. Chamorro, C. Hill, S. Morton, C. Ellis, R. Arndt, and F. Sotiropoulos, *On the interaction between a turbulent open channel flow and an axial-flow turbine,* Journal of Fluid Mechanics **716**, 658 (2013).